

Climatic and environmental changes in the Yana Highlands of north-eastern Siberia over the last *c.* 57 000 years, derived from a sediment core from Lake Emanda

MARLENE M. BAUMER, BERND WAGNER, HANNO MEYER, NIKLAS LEICHER, MATTHIAS LENZ, GRIGORY FEDOROV, LUIDMILA A. PESTRYAKOVA AND MARTIN MELLES

BOREAS



Baumer, M. M., Wagner, B., Meyer, H., Leicher, N., Lenz, M., Fedorov, G., Pestryakova, L. A. & Melles, M. 2021 (January): Climatic and environmental changes in the Yana Highlands of north-eastern Siberia over the last *c.* 57 000 years, derived from a sediment core from Lake Emanda. *Boreas*, Vol. 50, pp. 114–133. <https://doi.org/10.1111/bor.12476>. ISSN 0300-9483.

The sediment succession of Lake Emanda in the Yana Highlands was investigated to reconstruct the regional late Quaternary climate and environmental history. Hydro-acoustic data obtained during a field campaign in 2017 show laminated sediments in the north-western and deepest (up to ~15 m) part of the lake, where a ~6-m-long sediment core (Co1412) was retrieved. The sediment core was studied with a multi-proxy approach including sedimentological and geochemical analyses. The chronology of Co1412 is based on ¹⁴C AMS dating on plant fragments from the upper 4.65 m and by extrapolation suggests a basal age of *c.* 57 cal. ka BP. Pronounced changes in the proxy data indicate that early Marine Isotope Stage (MIS) 3 was characterized by unstable environmental conditions associated with short-term temperature and/or precipitation variations. This interval was followed by progressively colder and likely drier conditions during mid-MIS 3. A lake-level decline between 32.0 and 19.1 cal. ka BP was presumably related to increased continentality and dry conditions peaking during the Last Glacial Maximum (LGM). A subsequent rise in lake level could accordingly have been the result of increased rainfall, probably in combination with seasonally high meltwater input. A milder or wetter Lateglacial climate increased lake productivity and vegetation growth, the latter stabilizing the catchment and reducing clastic input into the lake. The Bølling-Allerød warming, Younger Dryas cooling and Holocene Thermal Maximum (HTM) are indicated by distinct changes in the environment around Lake Emanda. Unstable, but similar-to-present-day climatic and environmental conditions have persisted since *c.* 5 cal. ka BP. The results emphasize the highly continental setting of the study site and therefore suggest that the climate at Lake Emanda was predominantly controlled by changes in summer insolation, global sea level, and the extent of ice sheets over Eurasia, which influenced atmospheric circulation patterns.

Marlene M. Baumer (baumermarlene@googlemail.com), Bernd Wagner, Niklas Leicher, Matthias Lenz and Martin Melles, Institute of Geology and Mineralogy, University of Cologne, Zùlpicher StraÙe 49a, Cologne 50674, Germany; Hanno Meyer, Department of Periglacial Research, Alfred Wegener Institute, Helmholtz Centre for Polar and Marine Research, Research Department Potsdam, Telegrafenberg A43, Potsdam 14473, Germany; Grigory Fedorov, Geomorphology Department, Institute of Earth Sciences, St. Petersburg State University, Universitetskaya Nab. 7/9, St. Petersburg 199034, Russia and Department of Geography of Polar Regions, Arctic and Antarctic Research Institute, Bering Str. 38, St. Petersburg 199397, Russia; Luidmila A. Pestryakova, Institute of Biochemistry and Biology, North-Eastern Federal University of Yakutsk, Belinsky St. 58, 677000 Yakutsk, Russia; received 8th June 2020, accepted 10th August 2020.

Yakutia is known for its extremely continental climate, with the lowest temperatures of the Northern Hemisphere of -67.6 and -67.7 °C being recorded in the cities of Verkhoyansk and Oymyakon, respectively (Stephanova 1958). The most striking geomorphological feature of Yakutia is the Verkhoyansk Mountains, bordered by the Lena River valley to the west and the Yana Highlands to the east (Fig. 1A).

Our understanding of the palaeoenvironmental history of this area is based on a limited number of lacustrine sediment cores, permafrost or ice-complex sequences, and geomorphological archives (e.g. Müller *et al.* 2010; Stauch & Lehmkuhl 2010; Werner *et al.* 2010; Andreev *et al.* 2011; Biskaborn *et al.* 2016; Diekmann *et al.* 2017). Most of the lacustrine archives are located on the western margin of the Verkhoyansk Mountains (e.g. Biskaborn *et al.* 2016). One of the most detailed sedimentary records of climatic and environmental

change originates from Lake Billyakh in the south-western Verkhoyansk Mountains (Fig. 1A) and covers the last *c.* 50 cal. ka BP continuously (Müller *et al.* 2009; Tarasov *et al.* 2013; Diekmann *et al.* 2017). At the southern end of the Chersky Range, a palynological study on Lake Smorodinovoye (Fig. 1A) provides information on environmental change over the last *c.* 28 cal. ka BP (*c.* 24 ¹⁴C ka BP; Anderson *et al.* 2002; Andreev & Tarasov 2013). The Batagay permafrost sequence in the Yana Highlands (Fig. 1A) provides sparse information on the climate and vegetation history between Marine Isotope Stage (MIS) 6 (likely pre-MIS 6) and 2 (Ashastina *et al.* 2018; Opel *et al.* 2019). Ice-complex sequences found in coastal areas of the Laptev Sea (e.g. Andreev *et al.* 2011; Schirmermeister *et al.* 2017; Fig. 1A) provide climatic and environmental information back to *c.* 200 ka, but these archives are discontinuous and influenced by the proximity of the ocean.

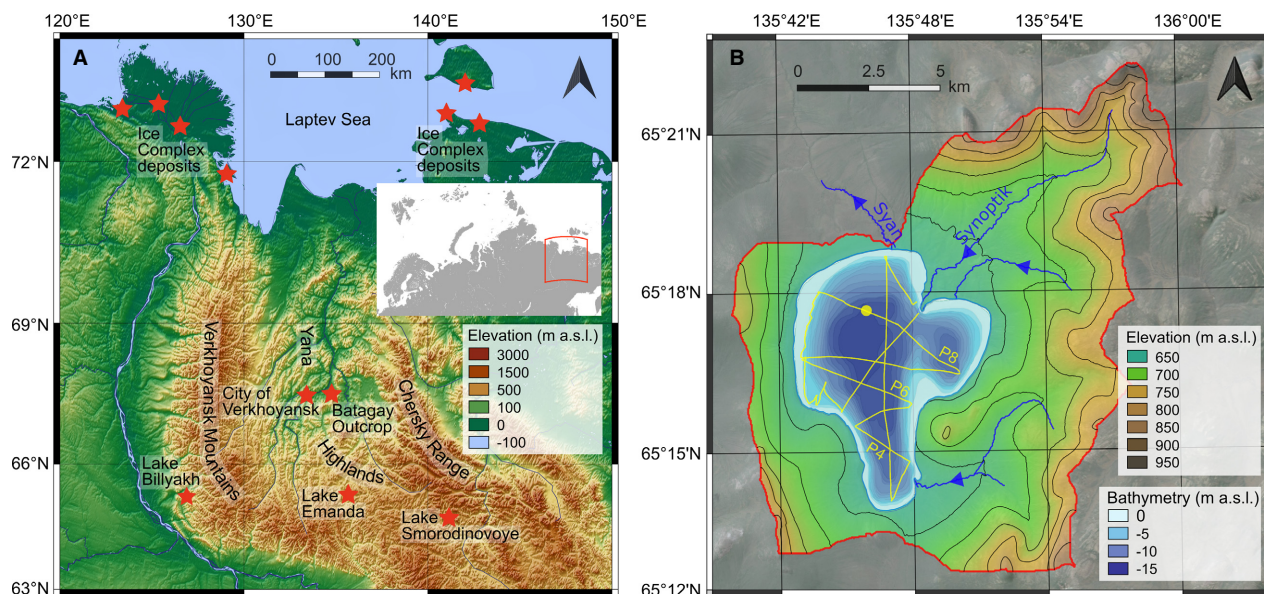


Fig. 1. Maps of the study area. A. Topographic map of northern and central Yakutia with its location in the Northern Hemisphere (red rectangle in the small overview map). The location of Lake Emanda and other locations mentioned in the text are marked with red stars. B. Topographic map of the catchment of Lake Emanda (red line) and its bathymetry (SURFER, Golden Software). Yellow lines mark the hydro-acoustic profiles acquired with an Innomar sediment echo-sounder. P4, P6 and P8 indicate the hydro-acoustic profiles shown in Fig. 2 and the yellow dot displays the location of sediment core Co1412. [Colour figure can be viewed at www.boreas.dk]

Information concerning the glaciation history of the Verkhoyansk Mountains was obtained by geomorphological mapping and infrared-stimulated luminescence (IRSL) dating of terminal moraines in this area (Popp *et al.* 2007; Stauch *et al.* 2007; Stauch & Gualtieri 2008; Stauch & Lehmkuhl 2010, 2011). The geochronological data from the Tumara and Djanushka valleys near Lake Billyakh document glaciations during MIS 6, MIS 5d, MIS 5b or MIS 4, sometime during late MIS 4, and early MIS 3 (not precisely dated; Stauch *et al.* 2007; Stauch & Gualtieri 2008; Stauch & Lehmkuhl 2010, 2011; Zech *et al.* 2011). During the cold stage of the LGM, only alpine glaciers developed (Stauch & Lehmkuhl 2010). This distinguishes the glaciation of the Verkhoyansk Mountains from northern Europe, where the Scandinavian Ice Sheet (SIS) had its maximum extent during the LGM (Svendsen *et al.* 2004; Stauch & Lehmkuhl 2010; Hughes *et al.* 2016). The SIS at this time bound moisture from predominantly westerly winds (Stauch & Lehmkuhl 2010) and blocked these air masses, leading to increasing aridity and limited glaciation further east (e.g. Krinner *et al.* 2011). Solar insolation, albedo, and topographic controls are discussed as additional drivers of asynchronous glaciation (Barr & Clark 2012). The importance of moisture sources is also evident in the regions further east (Anadyr, Koryak Mountains and Kamchatka), where precipitation from the Pacific Ocean controls the timing and extent of glaciation (Stauch & Gualtieri 2008; Stauch & Lehmkuhl 2010; Zech *et al.* 2011; Barr & Clark 2012; Elias & Brigham-Grette 2013).

Overall, the poorly investigated continental inland area of the Yana Highlands limits our understanding of the complex late Quaternary climatic and environmental history and the potential west to east gradients. Here, we present hydro-acoustic and sediment core data from Lake Emanda located ~270 km south-east of the city of Verkhoyansk (Fig. 1A) in order to (i) document the local climatic and environmental late Quaternary history by reconstructing short- and long-term changes in the lake and its catchment, and (ii) better understand the influence of North Atlantic air masses on regional precipitation compared to other records in the adjacent areas.

Regional setting

Lake Emanda is a heart-shaped lake in the Yana Highlands at 671 m above sea level (a.s.l.) (Fig. 1). The lake is 7.5 km long, 6.5 km wide, has a surface area of 33.1 km², and a maximum water depth of ~15 m (Fig. 1B). The main tributary, the Synoptik River, forms a delta in the north-eastern part of the lake. A second inflow, fed by small creeks from the surrounding 800–1000 m high mountains, forms a small delta in the south-east (Fig. 1B). The Syan River drains the lake in the north.

The climate at Lake Emanda is categorized as continental subarctic (Köppen 2011), with large seasonal temperature gradients and a mean annual precipitation of 233 mm (New *et al.* 2002). The present-day winter climate is predominantly controlled by the intensity of

the Siberian High Pressure system, which causes very cold and long winter periods with thin snow cover and mean January air temperatures of $-47.2\text{ }^{\circ}\text{C}$ (Barr & Clark 2012). The summer climate is mainly controlled by the Asiatic Thermal Low Pressure system and a high pressure system over the North Pacific, resulting in short but relatively warm summer periods with mean July temperatures of $13.1\text{ }^{\circ}\text{C}$ and higher precipitation of 40–50 mm per month between June and August (New *et al.* 2002). The modern-day growing season probably lasts from May to September, when monthly temperatures are above freezing and precipitation is increased. Nowadays, the moisture supply to the study area is mainly provided by winds from the North Atlantic, North Pacific, and partly from the Arctic Ocean (Stauch & Gualtieri 2008), with up to 40% of the moisture coming from the east, ~20–30% from the west and ~20–30% from the north (Papina *et al.* 2017). Significant contributions from both eastern and western moisture sources are confirmed by a backward trajectory model study for the Lena River delta in northern Siberia (Bonne *et al.* 2020). Only a few, typically cirque-type glaciers are currently found in the Verkhoysk Mountains (Koreisha 1991; Ananicheva & Krenke 2005; Stauch 2006; Glushkova 2011) and in the Chersky Mountains (Barr & Clark 2012; Fig. 1A), but none occurs in the catchment of Lake Emanda. The soil around the lake is pervaded by permafrost. The modern vegetation is represented by sparse mountain larch (*Larix cajanderi*) forests of lichen (*Flavocetraria cucullata*, *Cladina arbuscula*) type with *Betula exilis* and *Pinus pumila* and of *Vaccinium* - moss and lichen type (*V. vitis-idaea*, *V. uliginosum*, *Aulacomnium turgidum*, *Sphagnum* spp., *Flavocetraria cucullata*). The bedrock in the catchment of Lake Emanda (~179 km²; Fig. 1B) predominantly consists of Triassic to Jurassic, carbonate-bearing conglomerate, siltstone and sandstone (Dushin *et al.* 2009). The Yana Highlands are part of the Verkhoysk-Chukotka orogenic zone, which formed in Mesozoic times, when the Siberian Craton collided with the Kolyma-Omolon Microcontinent (Parfenov 1991; Oxman 2003).

Material and methods

Field work

A field campaign to Lake Emanda was carried out in August 2017. For mapping of the lake bathymetry and sediment architecture, a hydro-acoustic survey along 10 profiles (Fig. 1B) was conducted with an Innomar sediment echo-sounder (Innomar SES-2000 compact) operated at 10 kHz. A total of 37 km of hydro-acoustic profiles were processed with the Innomar ISE 2.9.5 software. Surfer 13 (Golden Software, USA) was used to create a bathymetric contour map (Fig. 1B). A coring location (latitude $65^{\circ}17.649'\text{N}$, longitude $135^{\circ}45.554'\text{E}$) was selected in the western lake basin at a water depth of

14.6 m (Figs 1B, 2), where the hydro-acoustic data show horizontal and parallel reflectors. Coring at this site Co1412 was conducted from a floating platform (UWITEC Ltd., Austria). Surface sediments down to 0.62 m below lake floor (b.l.f.) were recovered with a UWITEC gravity-corer (Co1412-1). Sediments down to 6.06 m b.l.f. were retrieved in up to 3-m-long and 0.5-m overlapping sediment sections (Co1412-3, -4 and -5) using a UWITEC piston corer. The uppermost 0.44 m of section Co1412-4, starting at 2.55 m b.l.f., consisted of sand, which was lost during core handling on deck. The sediment sections were cut into up to 1-m-long segments and transported to the University of Cologne for further analyses.

Sedimentological and geochemical work

In the laboratory, the sediment cores were split lengthwise and described for colour, grain size, structures, and carbonate content.

X-ray fluorescence (XRF) scanning was carried out on one of the core halves at 2-mm resolution using an ITRAX core scanner (Cox Analytical, Sweden) equipped with a chromium (Cr) tube. The scans were run with an integration time of 20 s, a voltage of 30 kV, and amperage set to 55 mA. The XRF data were processed with the QSpec 6.5 software (Cox Analytical, Sweden). Outliers at the core ends were removed from the data set. Titanium (Ti) was used to normalize the XRF data, because of its abundance, conservative nature during transport, and weathering combined with negligible biological importance (Löwemark *et al.* 2011).

The individual core segments were correlated to a core composite based on visual correlation of prominent layers as well as XRF element data using the Corewall software package (Correlator 1.696 and Corelyzer 2.0.1). One of the core halves from each segment was continuously subsampled in 1-cm sections. The water content was calculated from the weight-loss after freeze-drying the samples. For grain-size analysis, a sample aliquot of ~1 g of every fourth sample was pretreated with 10% hydrochloric acid (HCl), 35% hydrogen peroxide (H₂O₂) and 1 M sodium hydroxide (NaOH) to remove carbonate, organic matter (OM) and biogenic silica. Na₄P₂O₇ was added for sample dispersion prior to the measurement. A LS 13 320 Laser Diffraction Particle Size Analyser (Beckman Coulter, Germany) was used to measure the grain-size distributions; the GRADISTAD v.8.0 program (Blott & Pye 2001) was used for data processing. The grain-size results are given as volume percentages of the different particle diameter classes.

Approximately 100 mg of each sample was homogenized and ground to <63 μm for total nitrogen (TN), total sulphur (TS), total carbon (TC) and total inorganic carbon (TIC) measurements. TN and TS were measured with a Vario MICRO Cube elemental analyser (Elementar Corp., Germany) after combusting the material in small tin capsules at 1150 °C. A DIMATOC 2000 carbon

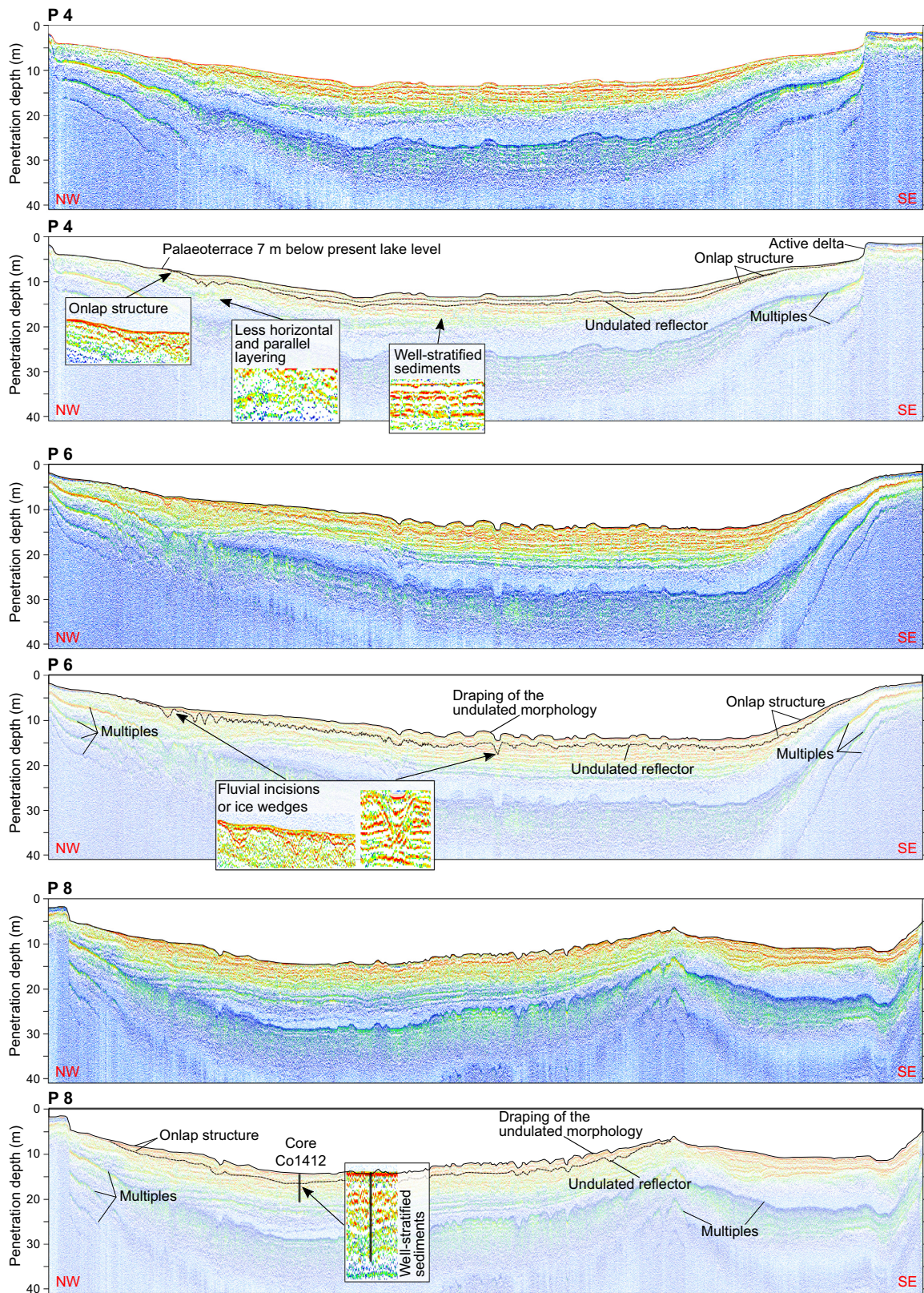


Fig. 2. Uninterpreted and interpreted hydro-acoustic profiles P4, P6 and P8 from Lake Emanda (for locations see Fig. 1B). The profiles illustrate the geometry of the lake basin as well as key stratigraphical characteristics of the sediment infill. P8 crosses the coring site Co1412. The black bar at site Co1412 indicates the approximate penetration depth. [Colour figure can be viewed at www.boreas.dk]

analyser (Dimatec Corp., Germany) was used to measure TC after combusting the material at 900 °C and TIC after pretreatment with phosphoric acid (H₃PO₄) and combustion at 160 °C. Total organic carbon (TOC) resulted from subtracting TIC from TC. The TOC/TN ratio was calculated from the TOC and TN contents using a factor of 1.167 to obtain the atomic ratio (Meyers & Teranes 2001). The minerogenic origin of TIC was checked in selected samples under a scanning electron microscope (SEM).

To analyse the carbon isotopic composition of every fourth sample, a sample aliquot of ~0.5 g was homogenized and treated with HCl to remove TIC. The samples were weighed into tin capsules and combusted at 1020 °C using a Thermo Fisher Scientific Delta-V-Advantage gas mass spectrometer equipped with a FLASH elemental analyser EA 2000, a CONFLO IV gas mixing system and an MA200R autosampler system at the Alfred-Wegener-Institute in Potsdam. The carbon isotope ratio is determined relative to laboratory standards of known isotopic composition and reported as delta values relative to the VPDB standard ($\delta^{13}\text{C}$) in per mil (‰) notation. The standard deviation (1 σ) is generally lower than $\delta^{13}\text{C} = \pm 0.15\%$.

Dating and age modelling

Dating of the sediment succession Co1412 focused on ¹⁴C dating, as other methods, such as biostratigraphy, palaeomagnetic measurements and luminescence dating, failed or are not available at the present time. For ¹⁴C dating, 13 samples throughout the sediment succession were sieved at >63- μm mesh size to extract plant fragments (Table 1). The extracted plant remains were too small for taxa identification and might therefore include terrestrial and aquatic remains. Chemical pretreatment and graphitization of samples COL5847 to COL5853 followed the standard protocol of Rethemeyer *et al.* (2013). For sample sizes <250 μg (COL5517 to COL5522) the extraction time was reduced and no alkali extraction applied (Rethemeyer *et al.* 2013). These samples were accordingly combusted and graphitized with an advanced version of the automated graphitization equipment (AGE) system coupled with an Elementar Analyser (EA; VarioMicroCube, Elementar, Germany) to avoid further loss of sample material (Rethemeyer *et al.* 2013). ¹⁴C dating was performed by accelerator mass spectrometry (AMS) at the University of Cologne Center for AMS (Dewald *et al.* 2013). Two sample aliquots, one of sample COL5847 and one of sample COL5852, were used for control measurement at the BETA Analytical Radiocarbon Dating Laboratory (Miami, Florida, USA) after pretreatment following the standard Beta Analytical protocol. ¹⁴C dating on organic sediment was carried out on two additional horizons at the BETA Analytical Radiocarbon Dating Laboratory after pretreatment with acid washes.

An age-depth model was calculated in R version 3.4.1 (R Core Team 2017) using the Bacon 2.3.6 software package (Blaauw & Christen 2011) and the IntCal13 and NH1 post-bomb calibration curves (Hua *et al.* 2013; Reimer *et al.* 2013). The age-depth curve is based on five ¹⁴C dates on plant fragments and the modern sediment surface (AD 2017). Ages were extrapolated to the bottom of the core, anticipating a constant sedimentation rate derived from the lowest dated horizons used for the age-depth model. Calibrated ages are provided with 2 σ confidence intervals as cal. ka BP.

Published ages from other records, which are only given as ¹⁴C ages and do not exceed the limits of existing calibration, were calibrated using Calib 7.1 (Stuiver *et al.* 2020) and are provided as cal. ka BP. Radiocarbon ages exceeding the limits of existing calibration are given as radiocarbon ages in ka BP.

Results and discussion

Hydro-acoustic data

The hydro-acoustic data reveal that the lake is made up of a western and eastern lake basin with maximum water depths of ~15 and ~11 m, respectively (Fig. 1B). A rather flat lake floor and gentle slopes characterize the morphology of the entire lake, except in the north-east and the south-east, where river inflows have formed deltas. The deltas stand out for their distinct geometry with an elongated delta plain, which likely developed when riverine discharge was high (Penland & Kulp 2005).

The sub-bottom reflectors display the sediment architecture down to ~15 m b.l.f., where they are masked by multiples. Three hydro-acoustic profiles, P4, P6 and P8 (Fig. 2), were selected to illustrate distinct morphological features of the sedimentary architecture in the Emanda basin. In the central part of the basin (P6 and P8 in Fig. 2) the reflectors above the multiples show horizontal, parallel to subparallel layering, and relatively undisturbed sedimentation. Towards the lateral parts of the basin and in the southernmost profile P4, the corresponding reflectors show less horizontal and parallel layering, indicating more disturbed sedimentation. The high-amplitude character of the reflectors points to distinct changes in sedimentological conditions. Files give evidence of a strong, undulated reflector, which emerges at the sediment surface in water depths of ~5–7 m and can be traced to ~1.9 m b.l.f. at coring site Co1412 (P8; Fig. 2). The undulated appearance of this reflector indicates a high-energy depositional environment in the central part of the basin during the time of its formation, probably as a result of very shallow water or even (seasonally) subaerial exposure. As the underlying sediments show no evidence of tectonic activity, the distinct depressions of the strong reflector could have been formed by fluvial incisions when the lake level was low. They could alternatively be associated with the forma-

Table 1. Radiocarbon data obtained from core Co1412. The dating was performed at the University of Cologne Center for AMS (COL) and the BETA Analytical Radiocarbon Dating Laboratory (BETA). All samples were organic macro-remains, except for samples BETA506615 and BETA506616, which were organic sediment samples. Ages used for the age-depth curve are marked in bold. * = beyond calibration curve.

Label	Composite depth (m c.d.)	Method	Mass C (μg)	Uncalibrated ^{14}C age (a BP)	2 σ conf. interval (a BP)	Calendar age (cal. a BP)	2 σ conf. interval (a BP)
COL5517	0.515	EA-AMS	52	4695	167	5290	466
COL5518	0.985	EA-AMS	114	9269	285	10 190	476
COL5519	1.686	EA-AMS	94	14 592	540	17 070	663
COL5520	2.535	EA-AMS	18	19 804	1026	22 590	1113
BETA506615	2.535	AMS		27 720	140	31 440	570
COL5847	2.585	AMS	641	45 423	1480	48 900	3376
BETA528646	2.585	AMS		25 750	180	29 860	1056
COL5521	2.795	EA-AMS	61	31 375	238	35 220	1030
COL5848	2.865	AMS	303	44 198	442	47 380	2203
COL5849	3.06	AMS	443	45 769	363	49 300	1560
COL5522	3.07	EA-AMS	24	>35 000	428	>35 000	
BETA506616	3.455	AMS		32 400	220	36 280	1070
COL5850	3.865	AMS	320	39 299	321	43 040	1042
COL5851	4.16	AMS	733	48 128	2034	50 000	2085
COL5852	4.65	AMS	999	49 559	2402	N/A*	
BETA513327	4.65	AMS		39 810	410	43 400	1427
COL5853	5.025	AMS	613	46 886	1762	50 000	2612

tion of ice wedges, which can occur under shallow water when the lake-ice freezes to the bottom, or could have formed through frost cracking, when the sediment surface became seasonally subaerially exposed. Larger seasonal lake-level changes, with amplitudes of up to several metres, are likely to have occurred due to the continental setting of the lake and are presently documented e.g. further north at Lake Taymyr (Alexanderson *et al.* 2001). In both cases, the undulated appearance of this reflector indicates a period when the lake level was ~5–7 m lower compared to present conditions. In the vicinity of the coring site, hydro-acoustic data do not provide evidence of disturbance and rather show well-stratified sediments (Fig. 2). All profiles evidence onlap structures above this reflector, thus suggesting that a lake-level increase followed the lake-level lowstand. As the sediments above the strong reflection drape the undulated morphology, a calm depositional environment (Gebhardt *et al.* 2017; Lebas *et al.* 2019) with low sedimentation rates can be inferred since the lake-level rise.

Sedimentological and geochemical data

Core Co1412 has a composite length of 6.06 m, consists of fine-grained hemipelagic sediments, and includes a gap from 2.99 to 2.88 m composite depth (m c.d.; Fig. 3). Except for this gap, sediment colour and structure do not record any distinct lithological boundaries or major hiatuses. Based on lithological variations the sediment succession was divided into five units, units E (6.06–5.20 m c.d.), D (5.20–4.41 m c.d.), C (4.41–1.89 m c.d.), B (1.89–1.08 m c.d.) and A (1.08–0 m c.d.) (Fig. 3).

Unit E (6.06–5.20 m c.d.). – The basal unit E is characterized by a repeated colour change from brown to grey, a

diffusely layered to massive sediment appearance, and relatively high clay content (Fig. 3), including clay aggregates of a few millimetres at the bottom of the unit. The colour transition from grey to brown at 5.6 m c.d. seems sharp, whereas the transitions from brown to grey at 6.91 and 5.39 m c.d. are rather gradual. The brown (grey) intervals are associated with higher (lower) TOC, lower (higher) Mn/Fe, higher (lower) TOC/TN, lighter (heavier) $\delta^{13}\text{C}_{\text{org}}$, lower (higher) potassium to titanium ratio (K/Ti), lower (higher) sand and lower (higher) TIC (Fig. 3).

The repeated colour change points to highly variable environmental conditions. The brown sediment colour in combination with elevated TOC contents argue for increased deposition of finely dispersed OM from enhanced productivity in the lake and its watershed (Meyers & Ishiwatari 1993; Cohen 2003). Low Mn/Fe in the brownish sediment point to reducing bottom-water conditions (Davison 1993; Boyle 2002; Davies *et al.* 2015), which support OM preservation at the sediment–water interface as a result of restricted microbial activity. Higher TOC/TN ratios within these intervals indicate increased allochthonous OM input (Meyers 1997, 2003), probably because of a relatively dense vegetation cover in the lake catchment. In such conditions, a high proportion of isotopically relatively light, soil-derived CO_2 from root respiration and humic acid decomposition could have decreased the dissolved inorganic carbon (DIC) isotope composition in the lake water (Hammarlund 1993; Turney 1999; Balascio & Bradley 2012). This, in combination with preferential use of the lighter ^{12}C by algae during photosynthesis (Ariztegui & McKenzie 1995; Mayr *et al.* 2009), could explain more negative $\delta^{13}\text{C}_{\text{org}}$ values in unit E (Hammarlund 1993; Turney 1999; Balascio & Bradley 2012). Also, lower K/Ti ratios within

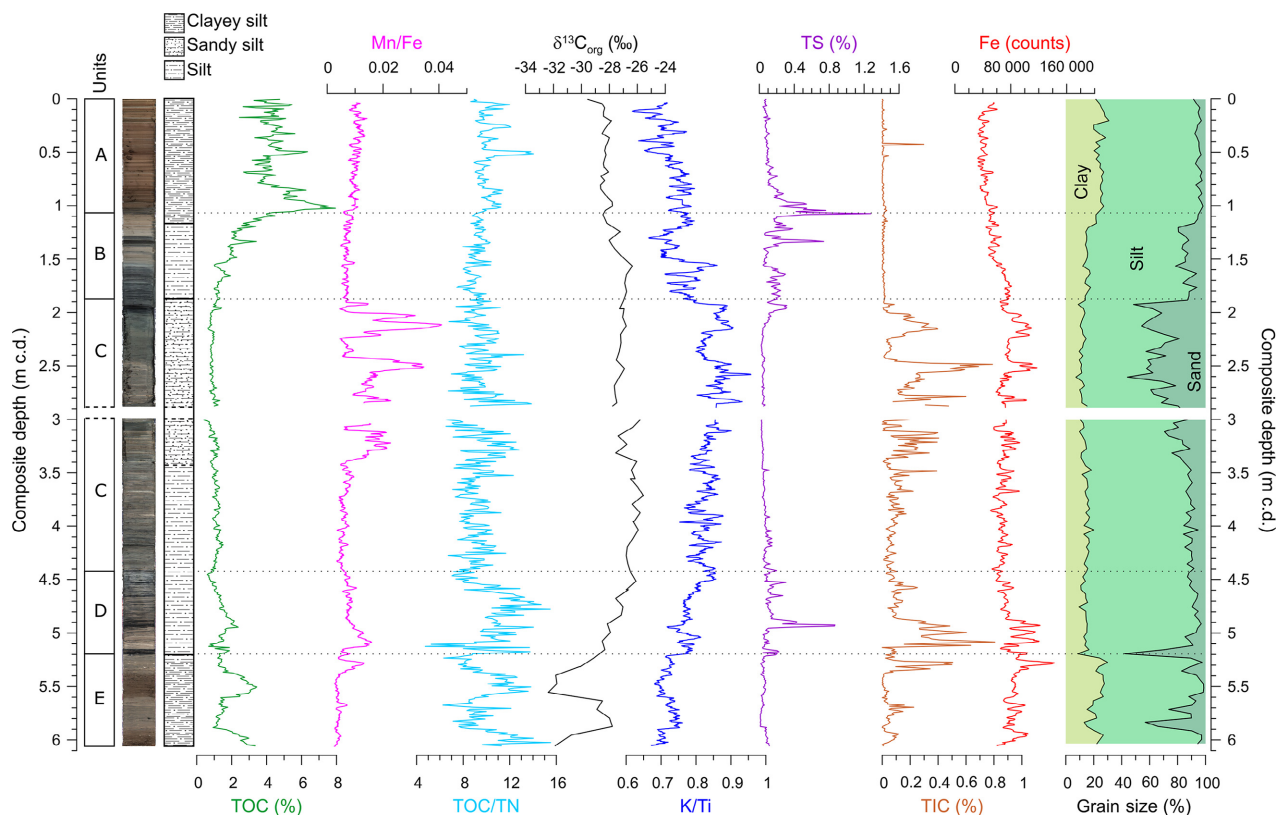


Fig. 3. Line-scan image, lithological subdivision and selected geochemical and physical parameters plotted against metres composite depth (m c.d.) of core Co1412. TOC, TIC and TS data are presented at 1-cm resolution, grain-size data are presented at 4-cm resolution, XRF core scanning data with an original resolution of 1 mm are smoothed by a 9-point running average. [Colour figure can be viewed at www.boreas.dk]

these intervals support the interpretation of a relatively stable landscape with relatively dense vegetation cover and well-developed soils, as they suggest that clastic matter leached of K by pedogenic processes was supplied to the lake (Arnaud *et al.* 2012; Francke *et al.* 2016, 2019). The lower TIC and sand contents within the brown intervals indicate reduced minerogenic input including detrital carbonate (checked with SEM) from carbonate weathering in the lake catchment, and restricted transport energy of the inlet streams, both potentially supported by a relatively dense vegetation cover.

In contrast, the grey horizons show lower OM, probably as a result of restricted lake and catchment productivity and increased decomposition caused by more oxic bottom-water conditions. A less dense vegetation cover and limited soil development allowed for enhanced minerogenic input, as indicated by higher K/Ti. Distinct peaks in sand content are likely attributed to periods of high transport energy, which might be associated with periods of enhanced runoff from rainfall or snow-melt or with low lake level and relatively short distances from the coring location to the inlets. Strong correlation of TIC and Fe might evidence the formation of authigenic siderite (Francke *et al.* 2016), which can form diagenetically under

reducing conditions in the pore space of the surface sediments (Berner 1981; Cohen 2003). Yellowish to brown siderite and vivianite concretions, of which the latter show a characteristic colour change from white to blue after core opening (e.g. Wagner *et al.* 2000), occur irregularly throughout unit E.

The diffusely layered to massive sediment appearance in unit E indicates resuspension from vigorous bottom currents (Cohen 2003). Bioturbation under oxic conditions contradicts with overall low Mn/Fe (Meyers & Ishiwatari 1993; Meyers 1997; Cohen 2003), except from a peak at 5.3 m c.d. Despite the maxima in sand content, the relatively high clay content shows that also periods with low transport energy must have prevailed. Such conditions could establish during winter, when the lake is ice-covered. The highly consolidated clay aggregates at the bottom of the unit point to migration of sediment particles through the lake-ice cover (Francke *et al.* 2013). They might alternatively indicate cryogenic processes after sedimentation (Zhigarev & Bocharova 1978; Stewart & Hartge 1995), when the water depth was shallow and the talik thickness underneath the water body was significantly reduced (Yi *et al.* 2014).

Unit D (5.20–4.41 m c.d.). – Unit D displays a change in colour from light brown to grey towards the top, shows

distinct, black lamination and is marked by relatively low clay content (Fig. 3). Mn/Fe and TOC show maxima at around 5.1 and 4.9 m c.d., respectively, and decrease gradually above. TOC/TN fluctuates between 5 and 16, with a tendency to overall higher values. The $\delta^{13}\text{C}_{\text{org}}$ and K/Ti curves show similar increases towards the top of the unit. The prominent black layers coincide with TS peaks. TIC is highly fluctuating with relatively high values between 5.1 and 4.9 m c.d. (Fig. 3).

The changes in colour and TOC are likely related to changes in productivity and preservation of OM, with highest TOC where the black lamination occurs. The coinciding TS peak suggests bacterial sulphate reduction during decomposition of OM in anaerobic sediments (Urban *et al.* 1999; Wagner *et al.* 2000), which is supported by reducing bottom-water conditions, inferred from low Mn/Fe. The variations in TOC/TN suggest fluctuating input of terrestrial OM compared to autochthonous OM.

Increasing $\delta^{13}\text{C}_{\text{org}}$ and K/Ti point to gradually reducing vegetation cover and soil development. The relatively low clay content suggests increased in-lake transport energy, probably due to enhanced runoff from the inlet stream and/or a lower lake level and accordingly shorter distance between the coring location and the shore (Blott & Pye 2001; Davies *et al.* 2015). The relatively high TIC between 5.1 and 4.9 m c.d., in concert with high Fe, might be a result of temporarily high minerogenic input, as siderite or endogenic calcite from carbonate precipitation were not observed in this core section.

Unit C (4.41–1.89 m c.d.). – Unit C comprises grey sediments, which appear diffusely to well layered below 2.46 m c.d. and more massive above (Fig. 3). Low TOC, TOC/TN and TS prevail, along with relatively heavy $\delta^{13}\text{C}_{\text{org}}$ (Fig. 3). A prominent feature of unit C is a fluctuating, but gradual increase in sand content and the occurrence of sporadic pebbles above 3.4 m c.d. Sandy sediments caused the loss of material, which led to the gap at 2.99–2.88 m c.d. The variations in the sand content are positively correlated with Mn/Fe, K/Ti and TIC (Fig. 3).

The overall characteristics of unit C suggest that productivity was low, decomposition of OM high, vegetation cover sparse and soil development limited. The upward increase in K/Ti indicates that clastic matter from relatively young and chemically unweathered soil was supplied to the lake, particularly where TIC and sand maxima indicate increased minerogenic input. High TIC also derives from formation of siderite (checked with SEM). The change in sediment appearance, coarsening and occurrence of scattered pebbles points to an increase in transport energy within the lake basin associated with enhanced runoff of the inlet streams and/or a shorter distance between coring location and shoreline. Large-scale fluctuations in Mn/Fe indicate that bottom-water

oxygenation was unstable and that longer periods of poor mixing alternated with periods of well-oxygenated bottom waters. A positive correlation between Mn/Fe, sand and K/Ti indicates that mixing was probably promoted during periods of enhanced river inflow. The occasional occurrence of pebbles could also be explained by ice-rafted transport. However, the very continental setting of the lake fosters lake-ice cover in winter and ice break-up in summer under a wide range of climatic boundary conditions and thus would promote ice-rafted transport also for the other sedimentary units, which are devoid of pebbles.

Unit B (1.89–1.08 m c.d.). – Unit B displays a twofold change of dark grey intervals with distinct black laminae to beige, diffusely layered intervals (Fig. 3). The topmost 12 cm of the upper beige, diffusely layered interval turns into more brownish sediments. The sand content sharply decreases at the boundary between units C and B, where the hydro-acoustic data show a strong, undulated reflector (P8; Fig. 2), and further decreases above 1.2 m c.d. TOC increases exponentially to the top of unit B. TOC/TN and K/Ti are fluctuating but relatively low. $\delta^{13}\text{C}_{\text{org}}$ values are relatively heavy in the lower dark grey interval and decrease above. TS shows some distinct peaks, whereas Mn/Fe and TIC are low, and Fe is decreasing in unit B (Fig. 3).

The repeated colour change indicates fluctuations in the environmental conditions. TOC, $\delta^{13}\text{C}_{\text{org}}$ and K/Ti point to an overall increase in lake and catchment productivity, soil development, and vegetation growth. TOC/TN ratios below 10.5 indicate a relatively high proportion of autochthonous OM. The more brownish colour and the significant increase in TOC above 1.2 m c.d. suggest a distinct change in the environmental conditions. Overall low Mn/Fe and occasionally high TS suggest that bacterial sulphate reduction during decomposition of OM was high when bottom-water oxygenation was low. The grain-size distribution indicates a relatively calm depositional environment, particularly at the top of the unit. Low TIC and decreasing Fe suggest that the input of clastic matter was low.

Unit A (1.08–0 m c.d.). – Unit A consists of brownish, diffusely layered sediments with relatively high clay and very low sand contents (Fig. 3). A darker brown sediment colour at the bottom of the unit coincides with distinct peaks in TOC and TS. Above, TOC is overall high, but varying with slightly lower values between 0.80 and 0.55 m c.d. and slightly higher values above 0.55 m c.d. Mn/Fe is overall low, with a vague maximum in the upper 0.55 m c.d. TOC/TN fluctuates between 8 and 14. $\delta^{13}\text{C}_{\text{org}}$ and K/Ti are relatively low, as is TIC, except for a single spike at 0.43 m c.d. (Fig. 3).

The brown sediment colour and elevated TOC indicate overall high OM content in unit A, with a maximum at 1.02 m c.d. TOC/TN suggests a mixture of autochthonous and allochthonous OM input, with slight variations

in relative proportions. $\delta^{13}\text{C}_{\text{org}}$ and K/Ti point to a dense vegetation cover and well-developed soils in the catchment. These settings resulted in reduced minerogenic input into the lake, as suggested by low TIC and lowest Fe. This is supported by relatively high clay and lowest sand contents, indicating low transport energy of inlet streams or relatively large distance between coring location and shoreline. The low Mn/Fe indicates an overall restricted bottom-water oxygenation, which presumably hampered sulphide formation (Müller 2001; Wagner *et al.* 2009).

Chronology

Only five of the 17 obtained radiocarbon dates were included in the age-depth model (Table 1; Fig. 4). A series of seven samples, which were sieved, processed and measured at the Cologne laboratory facilities, showed AMS ^{14}C dates older than 40 ka (COL5847–COL5853), without chronological order and in strong disagreement with the BETA ages from the same horizons and overlying and underlying intervals. As the sample sizes were rather small, the results could be biased, because low OM contents may be more susceptible to redeposited OM from the watershed (Abbott & Stafford 1996; Björck & Wohlfarth 2002), or contamination during sample preparation and processing. Given that contamination with old carbon is much more common than contamination resulting in younger ages (Rothacker *et al.* 2013; Sirocko *et al.* 2013), it is assumed that the younger BETA ages are the better estimate of the time of deposition. Accordingly, the entire measurement series (COL5847–COL5853) was omitted from the age-depth model. The same applies to sample BETA528646 at 2.59 m c.d., as this sample was split from sample COL5847 after pretreatment. A further two ^{14}C ages at 2.80 and 3.07 m c.d. (COL5521, COL5522) had to be excluded, as they exceeded the EA-AMS detection limit of 30 ka.

Two samples at 2.54 (BETA506615) and 3.46 m c.d. (BETA506616) are organic sediment samples, of which the upper indicates an age difference of 6940 years compared to the radiocarbon age obtained on plant remains from the same depth (COL5520). The age difference could be related to a size-dependent trend, as organic sediment samples bear a higher risk of containing very small particles including planktonic and reworked material (Rothacker *et al.* 2013), as compared to OM samples sieved at >63- μm mesh size. The two organic sediment samples were consequently discarded from the age-depth model.

The remaining five radiocarbon ages obtained on plant remains were used along with the sediment surface, which is assumed to correspond with the year of core recovery, to construct an age-depth model (Fig. 4). Owing to the few dating points, the 95% confidence interval between dated horizons is relatively large. The

ages in the upper 2.54 m c.d. indicate a constantly low sedimentation rate of 0.1 mm a^{-1} , despite significant changes in the grain-size distribution in unit C. The upper part of the age-depth model is supported by a good correlation of the colour changes in core Co1412 with variations in the NGRIP oxygen isotope record (Fig. 4; Andersen Azuma, Barnola *et al.* 2004). Brownish or darker horizons with increased OM in core Co1412 correspond to periods with heavier $\delta^{18}\text{O}$, including the Holocene and the Bølling-Allerød warm phases, whereas grey intervals with decreased OM below and above the presumed Bølling-Allerød coincide with periods with lighter $\delta^{18}\text{O}$ in the NGRIP record, corresponding to the Oldest and Younger Dryas. The only presumably reliable age in the lower part of our age-depth model comes from 4.65 m c.d. (BETA513327) and is $43.4 \pm 1.4 \text{ cal. ka BP}$. The tie point indicates that the sedimentation rate remained extremely low and that the gap between 2.88–2.99 m c.d. comprises about 1000 years. As no further chronological information can be obtained on the basis of the available data, the sedimentation rate between the two deepest presumably reliable ages at 2.54 (COL5520) and 4.65 m c.d. (BETA513327) was linearly extrapolated to the core bottom, resulting in a basal age of *c.* 57 cal. ka BP at 6.06 m c.d. (Fig. 4).

This basal age would place the deposition of unit E into the early MIS 3. The sharp colour transition from grey to brown at 5.6 m c.d. but gradual transitions from brown to grey at 6.91 and 5.39 m c.d. in unit E (Fig. 3) indicate a sawtooth pattern, which is also characteristic of Dansgaard-Oeschger (D-O) cycles in records from the North Atlantic realm. Atmospheric links between the North Atlantic and eastern Russia climate have for instance been described by Müller *et al.* (2010), Prokopenko *et al.* (2001) and Vasil'chuk (2006), who correlated variations in pollen, fossil diatom and isotope data from the sedimentary records of Lake Billyakh and Baikal, and Siberian ice wedges, respectively, with D-O cycles and Heinrich events. Assuming that the sedimentation rate in unit E remained constantly low, it can be speculated that the periodicity in unit E is in accordance with millennial-scale variability during D-O cycle 17/16 to 15/14, during summer insolation maximum at the latitude of Lake Emanda (Fig. 4). A tentative correlation with the more pronounced D-O cycles 20 to 19 at the transition from MIS 5 to MIS 4 would require a hiatus or change in sedimentation rate to even lower values, which is not evident in the lithology, geochemical proxies or hydro-acoustic data. Such a hiatus could be related to a complete desiccation of the lake; a horizon with significant changes in grain size, but also with remains of plant macrophytes as they grow in the lake littoral zone or on the shore today, was, however, not observed. A mass movement deposit, which could possibly have transported sediments away from the coring position, is excluded by sediment coring in the deepest part of the lake and the hydro-acoustic data.

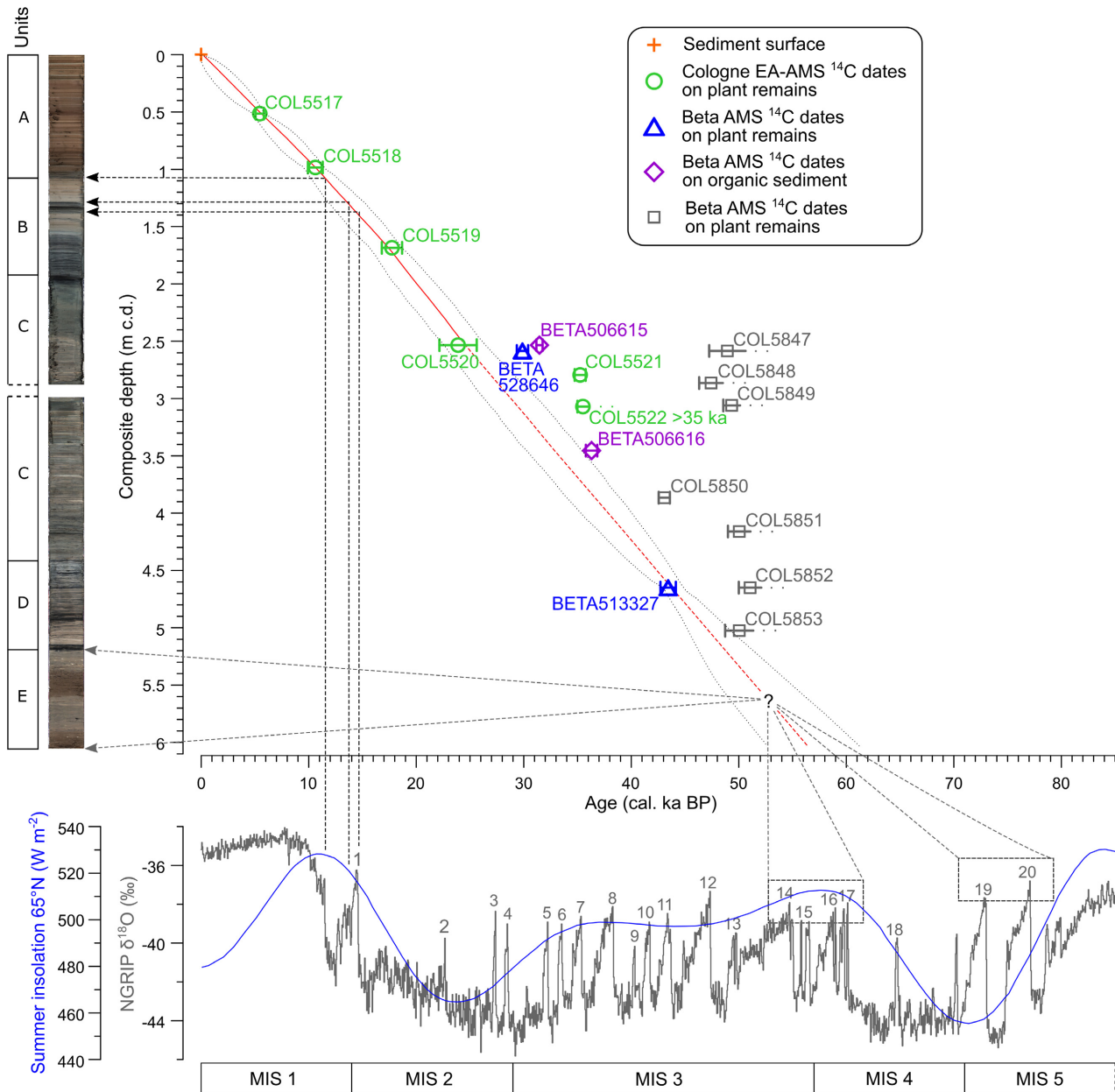


Fig. 4. Bayesian age-depth model of core Co1412, based on the modern sediment surface (AD2017) and five ^{14}C AMS dates on plant remains (COL5517–5520, BETA513327). Ages were calculated using the Bacon 2.3.6 graphsoftware package (Blaauw & Christen 2011). Individual ages are discussed in the text. Corresponding to the (low) high uncertainty of the curve progression in the upper (lower) part of the core, the age-depth curve is displayed with a solid (dashed) line. The comparison of colour changes in the Co1412 line-scan image and $\delta^{18}\text{O}$ NGRIP (grey line) with Dansgaard Oeschger (D-O) cycles (Andersen 2004) shows a good correlation around D-O 1 (Bølling-Allerød). The match of respective colour changes in the lower part of Co1412 with D-O 14-17 or D-O 19-20 is less well constrained and accordingly marked with a question mark. The summer insolation at 65°N (Berger & Loutre 1991) is also shown (blue line). [Colour figure can be viewed at www.boreas.dk]

Climatic and environmental history

Early MIS 3

As the chronology of the basal part of the Co1412 sediment succession is based entirely on extrapolated dates, we can only speculate about the timing of the alternating of brown and grey intervals in unit E and the

inferred strong fluctuations in the environmental and climatic conditions. According to our age-depth model, these fluctuations are constrained to early MIS 3 between c. 57 and 49 cal. ka BP.

Brown intervals with elevated OM and TOC/TN and relatively low $\delta^{13}\text{C}_{\text{org}}$ and K/Ti point to enhanced lake and catchment productivity, vegetation growth and soil development around the lake, which is interpreted to

reflect a moderately warm and/or humid spring to summer climate with relatively long growing seasons. Moderately warm summer temperatures likely promoted stratification of the water column, anoxic bottom waters and a better preservation of OM. Low sand and TIC contents suggest that the transport energy of the inlet streams and clastic matter input to the lake were restricted, probably as a consequence of a relatively dense vegetation cover. The highly consolidated clay aggregates at the bottom of the unit may have formed after deposition as a result of cryogenic processes after sedimentation, which would indicate a lower lake level sometime after the deposition of unit E.

Grey intervals with low OM and TOC/TN and increased Mn/Fe, $\delta^{13}\text{C}_{\text{org}}$ and K/Ti are, in contrast, associated with restricted lake and catchment productivity, limited soil development, and increased mixing of the water column and decomposition of OM, which is probably attributed to an overall colder and/or drier climate. Peaks in TIC and sand content indicate occasionally higher surface runoff and thus clastic input, which could be due to a less dense plant cover and/or periods of more frequent rainfall. Alternatively or additionally, the increased clastic accumulation could reflect a drop in the lake level, which cannot be verified by the hydro-acoustic data due to the low vertical resolution. Indications of a relatively low lake level are also given by the diffusely layered to massive sediment appearance and the overall low Mn/Fe in unit E, which imply that strong bottom currents or waves frequently resuspended the surface sediments.

The climatic instabilities could represent warmer/wetter and colder/drier periods during early MIS 3, when the summer insolation was relatively high (Berger & Loutre 1991; Fig. 5) and favourable for vegetation growth (Sher *et al.* 2005; Lozhkin & Anderson 2011; Ashastina *et al.* 2018). As a consequence of a relatively high summer insolation, evaporation can be assumed to have been increased, which would have shifted the water balance towards aridity (Kienast *et al.* 2005). At the same time, the global sea level fluctuated between ~50 and 80 m below the present level (Lambeck *et al.* 2002), which caused the exposure of large regions of the Bering Strait (Brigham-Grette *et al.* 2004) and a northward retreat of the shelf areas of the Laptev and East Siberian Seas by several hundred kilometres (Alekseev 1997; Lambeck *et al.* 2002; Brigham-Grette *et al.* 2004; Sher *et al.* 2005; Lozhkin & Anderson 2011; Opel *et al.* 2019). With larger extension of the Eurasian land surface and greater distance from the easterly and northerly moisture sources (Laptev, East Siberian and Bering Sea), the Yana Highlands supposedly experienced a more continental climate with increased summer-to-winter temperature amplitudes and decreased annual precipitation (Lambeck *et al.* 2002; Brigham-Grette *et al.* 2004; Sher *et al.* 2005; Lozhkin & Anderson 2011; Opel *et al.* 2019).

The observed fluctuations in environmental and climatic conditions at Lake Emanda could alternatively or additionally be attributed to waxing and waning of the SIS and the Barents-Kara Ice Sheet (BKIS) west of Lake Emanda (Knies *et al.* 2000; Svendsen *et al.* 2004, 2014; Stauch & Lehmkuhl 2010), which changed the pathways and intensity of moisture transport of the westerly wind system (Meyer *et al.* 2002; Lozhkin & Anderson 2011). Periods with occasionally high mean annual precipitation may also have promoted ice accumulation and maximum glacier extent at high elevations in the Verkhoyansk Mountains, as documented between 60–50 ka (Stauch *et al.* 2007; Zech *et al.* 2011).

Moreover, a supposed periodicity of *c.* 4000–5000 years of brownish (*c.* 57–55 and 52–50 cal. ka BP) to greyish (*c.* 55–52 and 50–49 cal. ka BP) horizons could indicate a link to D-O cycles in the North Atlantic region and related climatic instabilities (Fig. 4). Palaeodata and model simulations (CLIMBER-2) suggest that interstadial phases of D-O events are attributed to an increase in atmospheric precipitation at high northern latitudes (Prokopenko *et al.* 2001; Voelker 2002) and a northward shift of the intertropical convergence zone (Claussen *et al.* 2003). A climatic teleconnection could also exist via the intensity of the moisture-bearing East Asian summer monsoon, which correlates with North Atlantic temperatures between 75 and 11 ka BP (Wang *et al.* 2001; Bezrukova *et al.* 2010). However, the absence of other similar cycles in core Co1412 argues against a direct link to D-O events, as these events are most pronounced in the period between *c.* 60 and 30 ka BP in the North Atlantic records (Claussen *et al.* 2003) and could only be explained by major changes in atmospheric moisture pathways.

For a comparison of unit E with other records, the Batagay permafrost sequence, ~260 km to the north of Lake Emanda (Fig. 1A), provides the closest record including early MIS 3. In contrast to the reconstruction from Lake Emanda, this record suggests a generally stable, cold-stage early MIS 3 climate, which led to the formation of syngenetic ice-complex deposits (Ashastina *et al.* 2017, 2018; Opel *et al.* 2019). Ice-complex records from coastal areas of the Laptev Sea, >700 km to the north of Lake Emanda (Fig. 1A), which may have higher temporal resolutions, also indicate climatic conditions comparable to full-glacial time, with only subtle variations from colder/drier to slightly warmer/moister conditions at *c.* 50 ^{14}C ka BP (Schirmermeister *et al.* 2003; Andreev *et al.* 2009, 2011). The palaeoclimate interpretation from Lake El'gygytyn, ~1600 km to the east of Lake Emanda, is generally consistent with that from the Batagay and the Laptev Sea region, although it indicates a subtle shift from warmer to cooler/moister conditions at 54.1 ^{14}C ka BP (Lozhkin *et al.* 2007; Lozhkin & Anderson 2011). A record with higher amplitude climate variations during early MIS 3 comes from Lake Elikchan

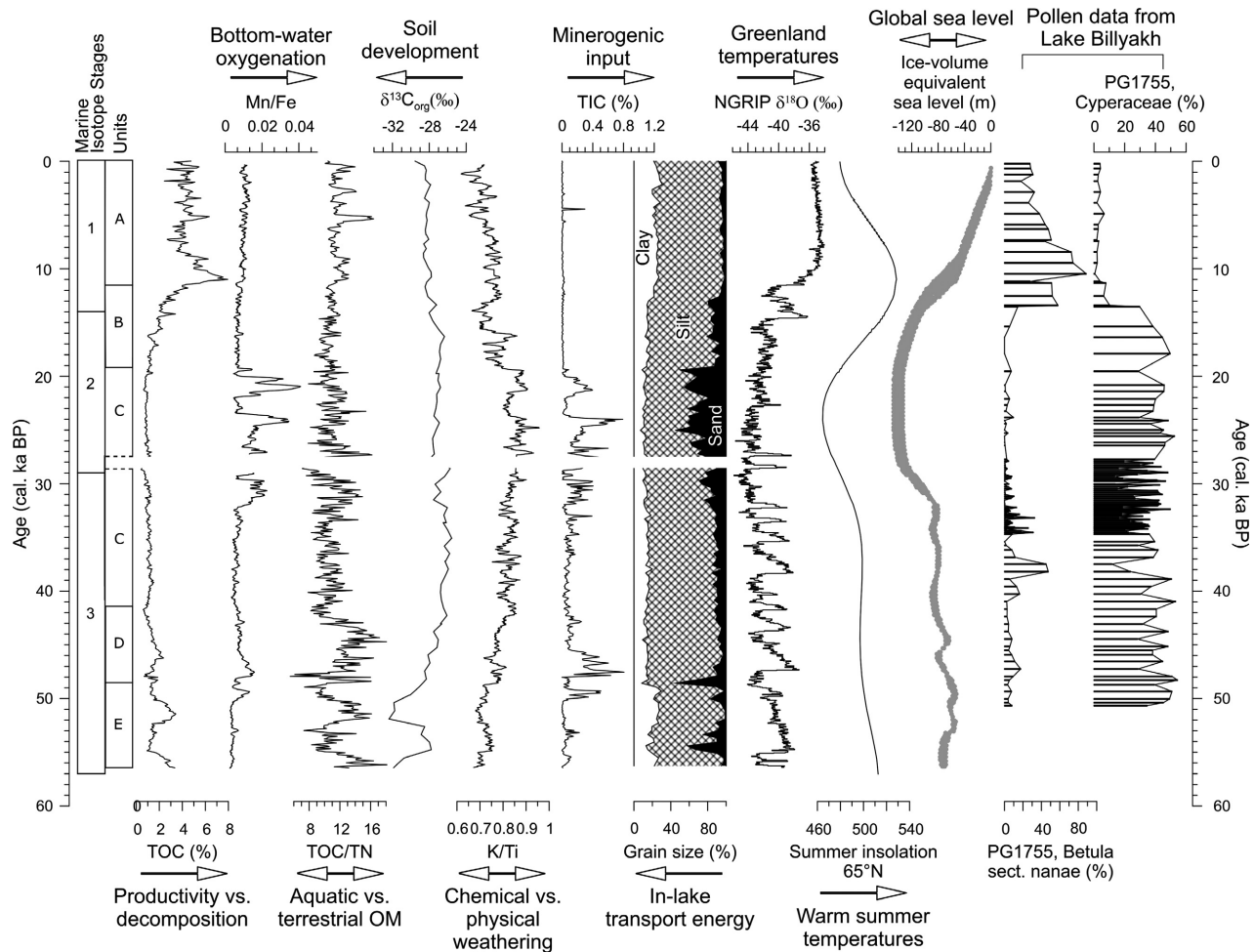


Fig. 5. Proxy data of core Co1412 plotted against age and compared to marine oxygen isotope stages (Lisiecki & Raymo 2005), NGRIP $\delta^{18}\text{O}$ data (Andersen 2004), the local (65°N) summer insolation (Berger & Loutre 1991), ice-equivalent sea level (Lambeck *et al.* 2002) and pollen data from Lake Billyakh (core PG1755; Müller *et al.* 2010). Grain-size data are accumulated clay, silt and sand fractions (from left to right). The K/Ti data with an original resolution of 1 mm are smoothed by a 9-point running average.

in the southern Magadan region (Kienast *et al.* 2005; Sher *et al.* 2005; Lozhkin & Anderson 2011), ~900 km to the south-east of Lake Emada. The Lake Elikchan record describes moderately warm/wet, cool/dry, moderately warm/dry and cool/dry conditions at 60–57.6, 55.6–53.4, 53.4–48.4 and 48.4–46.8 ^{14}C ka BP, respectively, in line with sea-surface temperatures fluctuations in the Okhotsk Sea (Gorbarenko *et al.* 2004). Stronger environmental shifts at Lake Elikchan and Emada could be due to similar forcing or feedback mechanisms, which Lozhkin & Anderson (2011) tentatively ascribed to D-O events. Climatic instabilities during the MIS 3 interstadial have also been discussed for different type sections in the Yana-Indigirka-Kolyma lowlands (Anderson & Lozhkin 2001; Zanina *et al.* 2011), although the exact temporal classification within the MIS 3 interstadial remains questionable (Anderson & Lozhkin 2001). The studies document relatively warm/humid intervals with summer temperatures rising to

nearly modern values and a northward migration of the tree line to approximately its present limit. The sediment record from Lake Billyakh (Müller *et al.* 2010), ~420 km west of Lake Emada (Fig. 1A), does not cover the entire period as presumably recorded in unit E. The vegetation reconstruction from the lowermost part of the Lake Billyakh record may roughly correspond to the grey interval between c. 50 and 49 ka BP in core Co1412. The climatic differences between the individual records are likely due to chronological uncertainties, but could also be caused by latitudinal differences between more southern or central sites, such as Lakes Elikchan and Emada, in contrast to the study sites in Batagay and the Laptev Sea coast further to the north.

Mid-MIS 3

The age-model suggests an accumulation of unit D between c. 49 and 41.3 cal. ka BP, hence during mid-MIS

3. The chronological information is based on the lowermost presumably reliable ^{14}C date of 43.4 cal. ka BP at 4.65 m c.d. (Fig. 4, Table 1). The TOC suggests a period of moderately warm and/or moist summers, which facilitated a slightly higher productivity around 46 cal. ka BP; and progressively colder and/or drier conditions than in unit E, expressed in a decrease in productivity thereafter. Increasing aridity would lead to thinner or lacking snow covers and, thus, to less protection of plants from very low winter temperatures (Kienast *et al.* 2005). The overall shift to lower productivity is consistent with lower mid-MIS 3 summer insolation (Berger & Loutre 1991), and accordingly shorter growing seasons and lower summer temperatures. A relatively high TOC/TN until 42.7 cal. ka BP suggests that aquatic productivity decreased, likely as a result of colder conditions and a shorter ice-free growing season. Increases in $\delta^{13}\text{C}_{\text{org}}$ and K/Ti point to more open ground and less soil development, which increased physical weathering. The distinct black lamination, which coincides with TS peaks and low Mn/Fe, suggests that the bottom waters were more anoxic when the ice-free period in summer was shorter. Elevated Mn/Fe and TIC between *c.* 48 and 46 cal. ka BP suggest a period of relatively high minerogenic input and oxygenation of the water column, likely due to high runoff. The relatively low clay proportion in the sediments indicates a higher transport energy regime, probably attributed to a relatively low lake level and increased water-current activity.

The sediment core from Lake Billyakh (Fig. 1A), the closest record that covers this time interval in great detail, points to considerably cold and dry conditions with the exception of a short-term episode of warmer and wetter conditions at *c.* 47.5 cal. ka BP (Müller *et al.* 2010). Overall, the climate reconstruction from Lake Billyakh suggests colder and drier conditions compared to Lake Emanda (Müller *et al.* 2010), a climatic state that contrasts with the present-day atmospheric circulation pattern, which causes more humid and less continental conditions on the western, windward side of the Verkhoysansk Mountains. The discrepancy between the two records can be explained by the occurrence of glaciers in the Djanushka River Valley, in the western Verkhoysansk Mountains (Diekmann *et al.* 2017), which repeatedly fed Lake Billyakh with glacial meltwater runoff (Diekmann *et al.* 2017). These regional glaciers were mainly confined to the western, windward side of the mountain range (Stauch & Lehmkuhl 2010; Barr & Clark 2012). The difference between the two records could as well suggest that the Yana Highlands and Lake Emanda were more strongly influenced by warm and humid air masses from the North Pacific than Lake Billyakh.

Ice-complex records from the Laptev Sea region suggest cold climate conditions with slightly moister and warmer summers (Andreev *et al.* 2011) and slightly warmer winters (Meyer *et al.* 2002; Andreev *et al.* 2009)

during mid-MIS 3 compared to the previous interval >50 ^{14}C ka BP, hence indicating a slight decrease in seasonality. At Lake El'gygytyn, a slight change from cooler/moister to nearly full-glacial conditions is indicated at 46.2 ^{14}C ka BP (Lozhkin *et al.* 2007; Lozhkin & Anderson 2011). These results suggest that the environments were less productive compared to Lake Emanda, where a wetter and more continental climate with relatively warm summer temperatures promoted productivity. The Lake Elikchan record in the southern Magadan region indicates generally warm temperatures and/or relatively high effective moisture after 46.8 ^{14}C ka BP, including an interstadial optimum with present-day vegetation 46.8–44.8 ^{14}C ka BP (Kienast *et al.* 2005; Lozhkin & Anderson 2011). Such climatic conditions are attributed to warm sea-surface temperatures in the Okhotsk Sea and the only moderate exposure of the shelf along the Chukotka and the Okhotsk Sea compared to the northern coast, making continentality negligible (Lozhkin & Anderson 2011).

Late MIS 3 and LGM

Unit C spans the time interval between 41.3 and 19.1 cal. ka BP, i.e. late MIS 3 and most of MIS 2, including the LGM (26.5–19 ka BP; Clark *et al.* 2009). As suggested by the grey sediment appearance and overall low TOC and TOC/TN, this period is associated with a persistently cold and dry climate and resultant low productivity environment at Lake Emanda. Less negative $\delta^{13}\text{C}_{\text{org}}$ values indicate that the nutrient supply from the catchment to the lake was minimized when the harsh climate conditions restricted soil development and supposedly limited plant communities to those adapted to colder and drier climate conditions. The relatively open vegetation enhanced physical weathering, as suggested by the upward increase in K/Ti.

The pronounced coarsening of the sediments between 32.0 and 19.1 cal. ka BP suggests an increase in surface runoff and/or a lake-level lowering and rerouting of the inlet streams towards the coring location. A lake level ~7 m lower than today is inferred by the undulated reflector in the hydro-acoustic data (Fig. 2), which supposedly formed during the lake-level lowstand around 19.1 cal. ka BP. The shape of the undulated reflector suggests that fluvial incisions or ice-wedge polygons formed during shallow water conditions or seasonal, subaerial exposure. The cold climate did not exclude transport of pebbles through lake-ice floes, as the continental setting of Lake Emanda likely fostered lake-ice melting in summer. Spring to summer melting of local snow fields and thawing of permafrost soils probably promoted surface runoff during pulsed meltwater discharges. This suggestion is supported by fluctuations in TIC and sand and the occurrence of scattered pebbles, which point to highly variable input from the inlet streams. Periods of highly energetic river input could

have led to the formation of the distinct geometry of the Synoptic delta distributary in the north-eastern part of the lake. High-amplitude fluctuations in Mn/Fe correlate well with the TIC maxima and high sand content, thus indicating that fluvial input events may have caused temporary bottom-water oxygenation.

The lowering of the lake level to a minimum around 19.1 cal. ka BP can be attributed to extremely dry climate conditions during the LGM, which probably caused a negative net water budget (Kienast *et al.* 2005). Such conditions during the LGM could have been promoted by the global sea-level minimum at about -120 m below present level (Fig. 5), which led to the extension of the northern shelf areas of ~700 km and a closed Bering Strait (Alekseev 1997; Lambeck *et al.* 2002; Brigham-Grette *et al.* 2004; Sher *et al.* 2005; Lozhkin & Anderson 2011; Opel *et al.* 2019). The relatively weak correlation between climatic change at Lake Emanda and $\delta^{18}\text{O}$ variations in Greenland (Fig. 4; Andersen *et al.* 2004) moreover indicates that the maximum extension the BKIS and SIS at that time restricted moisture transport by the westerly wind system from the North Atlantic and hence glaciations east of the SIS (Knies *et al.* 2000; Svendsen *et al.* 2004, 2019; Stauch & Lehmkuhl 2010; Tarasov *et al.* 2019). It also suggests that a strong Siberian High ensured cold and dry conditions by impeding moisture transport to North and Central Siberia during winter (Dale Guthrie 2001; Murton *et al.* 2015).

Comparing the record from Lake Emanda with other records from the surroundings reveals some smaller discrepancies, but an overall picture of regional aridity and cool conditions. The environmental reconstructions from the Batagay permafrost sequence further north (Fig. 1A) give no indication of short-term climatic fluctuations during this interval, but confirm that the Yana Highlands experienced a shift to extremely arid conditions at the onset of the LGM (Ashastina *et al.* 2018). In contrast, the Lake Billyakh record to the west (Fig. 1A) supposedly tracks D-O events expressed as short-term fluctuations in runoff (Diekmann *et al.* 2017) and changes in vegetation (Müller *et al.* 2010) at c. 38 and 33 cal. ka BP. After 30.9 cal. ka BP, the record documents a lake-level lowering and strong aeolian input as a result of coldest and driest conditions within the recorded period (Müller *et al.* 2010; Tarasov *et al.* 2013; Diekmann *et al.* 2017), which fits well with the data from Lake Emanda. A transition from partly warmer conditions with enhanced plant diversity and more continuous vegetation cover to full-glacial conditions until the end of the LGM was also reported from the Laptev Sea region, Lake El'gygytgyn, and the southern Magadan region at c. 39.6–34.1 cal. ka BP (35–30 ^{14}C ka BP) (Andreev *et al.* 2002, 2009, 2011; Lozhkin *et al.* 2007; Lozhkin & Anderson 2011). This emphasizes that the pronounced aridity reconstructed for Lake Emanda was a prominent regional signal.

Lateglacial

Unit B covers the interval between 19.1 and 11.6 cal. ka BP. The sharp decrease in sand content at 19.1 cal. ka BP and progressive onlap of all reflectors corresponding to unit B in the hydro-acoustic data of Lake Emanda likely indicate an increase of the lake level (Gebhardt *et al.* 2017; Lebas *et al.* 2019). The distinct increase in TOC suggests increasing productivity in the lake and its catchment in the course of Unit B deposition, which could be related to a wetter and milder climate and longer summer periods, especially towards the Pleistocene/Holocene transition, when more brownish sediments are observed. The relatively low TOC/TN suggests that aquatic productivity was relatively high, presumably due to a higher nutrient input into the lake, increased summer temperatures and longer ice-free growing seasons. The relatively low K/Ti, negligible TIC and decrease in sand content after 12.9 cal. ka BP suggest that an expanding vegetation cover stabilized the lake catchment and reduced clastic input. This corresponds well with the decrease in $\delta^{13}\text{C}_{\text{org}}$, which points to an increase in soil development after 16.4 cal. ka BP. As a result of the higher lake level and denser vegetation cover a calm depositional environment established. Overall low Mn/Fe and occasionally high TS suggest that mixing of the water column and oxygenation of the bottom water was restricted and bacterial sulphate reduction during OM decomposition fluctuated. The repeated colour changes in unit B indicate distinct changes in the environmental conditions with likely warmer and/or wetter conditions 19.1–16.4 and 14.7–13.8 cal. ka BP and cooler and/or drier conditions 16.4–14.7 and 13.8–11.6 cal. ka BP. Overall, the Lateglacial was a time of considerable climatic change with increasing terrestrial and aquatic productivity, landscape stabilization, and continued rise of the lake level as a consequence of increased effective moisture.

The observed environmental changes are synchronous with an increase in Northern Hemisphere summer insolation (Berger & Loutre 1991; Fig. 4), global sea-level rise (Lambeck *et al.* 2002; Brigham-Grette *et al.* 2004; Sher *et al.* 2005; Lozhkin & Anderson 2011) and retreat of glaciers in the Verkhoyansk Mountains (Kind 1975; Kolpakov & Belova 1980), the Polar Urals and Europe (Svendsen *et al.* 2004, 2014). The lake-level rise of Lake Emanda may therefore have been driven by the reduced distance to the moisture sources of the Yana Highlands, and/or increased moisture supply by warmer air masses. In addition, an increased meltwater supply and thermokarst activity during summer may have further added to the positive water balance. The distinct colour changes in the upper part of core Co1412 could correspond to climatic variations during the Bølling-Allerød warming and Younger Dryas cooling (Fig. 4; Andersen *et al.* 2004) documented in the NGRIP record

between 14.6 and 11.6 ka BP, respectively (Rasmussen *et al.* 2006). The inferred good correlation between climatic changes at Lake Emanda and $\delta^{18}\text{O}$ variations in Greenland (Fig. 4; Andersen *et al.* 2004) furthermore suggests that the climate in the Yana Highlands experienced a distinct influence of North Atlantic climate variability via the westerly wind system after the decay of the LGM ice sheets over Eurasia. The relatively high TOC content within this beige interval suggests that the climate during the Younger Dryas was less severe than prior to 14.7 cal. ka BP.

Compared to Lake Billyakh (Diekmann *et al.* 2017; Fig. 1A), Lake Emanda records milder and wetter conditions in the period 19.1 to 14.7 cal. ka BP. Cold conditions at Lake Billyakh during that period suggest that moisture from retreating glaciers in the Polar Urals and Europe did not reach Yakutia via the westerly wind system, probably because the ice sheets altered the pathways of moisture transport (Meyer *et al.* 2002). The discrepancy furthermore suggests that the Verkhoyansk Mountains as a morphological barrier prevented the transport of cold air masses to Lake Emanda. This relatively protected setting in the Yana Highlands, the increasing summer insolation, and reduced continentality probably also led to increased thermal erosion of the Batagay Ice Complex (Ashastina *et al.* 2017; Fig. 1A). Milder and wetter conditions following the LGM have also been reconstructed from ice-complex deposits in the Laptev Sea region to the north of Lake Emanda (Fig. 1A) after 20 cal. ka BP (Meyer *et al.* 2002) and 19.3 cal. ka BP (^{14}C ka BP; Andreev *et al.* 2011). Our climatic interpretation of a warmer and wetter Bølling-Allerød and cooler and drier Younger Dryas period is consistent with several palynological studies from adjacent regions (Andreev *et al.* 1997, 2011; Pisaric *et al.* 2001; Anderson *et al.* 2002; Müller *et al.* 2009; Andreev & Tarasov 2013). The rapid warming towards the Holocene, as recorded in core Co1412, is contemporaneous with the final cessation of the Batagay ice-complex deposits around 12 cal. ka BP (Ashastina *et al.* 2017). The associated decrease in runoff and/or increase of the Emanda lake level is in good accordance with the onset of a deep-lake stage of Lake Billyakh after 12 cal. ka BP (Diekmann *et al.* 2017).

Holocene

Unit A covers the Holocene period from 11.6 cal. ka BP until today, which is associated with a relatively warm and humid climate that allowed for a highly productive environment as suggested by brown sediment colour and overall high OM contents. A peak in productivity due to presumably warmer than present temperatures is indicated for the period 11.5–9.0 cal. ka BP by the dark brown sediment colour and highest TOC and TS. Relatively high TOC/TN and relatively low $\delta^{13}\text{C}_{\text{org}}$, K/Ti and TIC imply that the warming at the onset of the

Holocene led to increased vegetation cover and soil formation, which stabilized the catchment and restricted clastic input. This is supported by relatively high clay and lowest sand contents, indicating low transport energy of inlet streams and/or relatively deep waters at the coring location. Such settings may also have restricted mixing of the water column and bottom-water oxygenation, as suggested by overall low Mn/Fe. The slightly lower TOC but relatively high TS between 8.5 and 5.8 cal. ka BP indicate that bacterial sulphate reduction reduced the sedimentary OM content during this interval. Highly fluctuating TOC during the last 5.2 ka points to unstable but similar-to-present-day climatic and environmental conditions.

The beginning of the Early Holocene warming at 11.6 cal. ka BP at Lake Emanda coincides with the maximum in local insolation (Berger & Loutre 1991; Fig. 4) and is consistent with warming around Lake Billyakh at 11.3 cal. ka BP (Müller *et al.* 2009), in the Laptev Sea region at 11.5 cal. ka BP (Andreev *et al.* 2011) and at Lake El'gygytgyn at 12 cal. ka BP (Swann *et al.* 2010). Pollen-based climate reconstructions from the Laptev Sea region inferred temperatures 4 °C warmer than today for the interval 11.5–8.4 cal. ka BP (Andreev *et al.* 2011), corresponding to the Holocene Thermal Maximum (HTM) at Lake Emanda at 11.5–9.0 cal. ka BP and at Lake El'gygytgyn at 11.4–7.6 cal. ka BP (Swann *et al.* 2010). At Lake Billyakh and Lake Smorodinovoye (Fig. 1A) maximum post-glacial warming, however, occurred after 7 cal. ka BP, which rather corresponds to a HTM timing between 8 and 6 cal. ka BP from Lake Baikal in central Eurasia (Demske *et al.* 2005; Müller *et al.* 2009; Swann *et al.* 2010). According to global climate models, the delayed onset of the HTM at more southerly locations can be explained by the deglaciation of Laurentide Ice Sheet remnants, which brought cold air to more central and southern sites of Eurasia until 7 cal. ka BP (Renssen *et al.* 2009, 2012; Biskaborn *et al.* 2016), while northern sites remained unaffected by this process. The asynchronous timing of the HTM could also be a response to increasing continentality and a decreasing contrast of seasonal insolation over the course of the Holocene, which varies regionally (Laskar *et al.* 2004; Subetto *et al.* 2017). The establishment of unstable, but similar-to-modern environments during the Middle to Late Holocene, as recorded at Lake Emanda, has also been reported from other sites such as Lake Nikolay (Andreev *et al.* 2004).

Conclusions

Hydro-acoustic investigations as well as multi-disciplinary studies of the 6.06-m c.d.-long sediment core Co1412 from Lake Emanda revealed new insights into the late Quaternary climate and environmental history of the Yana Highlands.

- The basal age of core Co1412 was determined by downward extrapolation of the sedimentation rate and suggests continuous lacustrine sedimentation since c. 57 cal. ka BP.
- The lowermost sediments indicate repeated shifts between supposedly warmer/wetter and colder/drier conditions, which may have occurred during early MIS 3. This period was followed by a decrease in productivity probably due to progressively colder/drier conditions during mid-MIS 3. A relatively harsh climate is indicated during late MIS 3 and towards the LGM that was associated with a significant lowering of the lake level between 32.0 and 19.1 cal. ka BP. A subsequent lake-level increase may be attributed to slightly warmer/moister conditions at Lake Emanda during the Lateglacial. The Bølling-Allerød and Younger Dryas periods indicate warmer/wetter and cooler/drier conditions, respectively. An Early Holocene warming at 11.6 cal. ka BP and the HTM between 11.5 and 9.0 cal. ka BP were followed by a transition to an unstable but similar-to-modern environment after 5.0 cal. ka BP.
- The observed climatic and environmental fluctuations are presumably controlled by (i) the pronounced continental setting of Lake Emanda, (ii) changes in summer insolation, which controls the length of the growing season and amount of meltwater supply during summer, (iii) oscillations of the global sea level, which changes the degree of continentality in the Yana Highlands and the maritime moisture convergence from the east and north, (iv) the extent of Eurasian ice sheets (SIS and BKIS), which changes the pathways of moisture-laden air masses from the west, and (v) a distinct influence of North Atlantic climate changes supposedly at the beginning of MIS 3 and at the Pleistocene/Holocene transition.
- According to the hydro-acoustic data, at least eight additional metres of stratified sediments could be retrieved before reaching the bedrock. Lake Emanda therefore has a great potential to be amongst the very few lakes in northern Russia that contain a continuous sediment succession back to the Eemian or even beyond.

Acknowledgements. – Financial support for this study was provided by the German Federal Ministry of Education and Research (BMBF; grant no. 03F0830A). The work of L. Pestryakova was sponsored by the Russian Foundation for Basic Research (grant no. 18-45-140053 r_a) and the Russian Ministry of Education and Science (FSRG-2020-0019). We are grateful to various colleagues from the North-Eastern Federal University in Yakutsk for their logistical help during the fieldwork in summer 2017. We also acknowledge Dima Bolshiyarov from the Arctic and Antarctic Research Institute in St. Petersburg for his participation in the field campaign. Nicole Mantke and Dorothea Klinghardt from the University of Cologne are acknowledged for their assistance during laboratory work. We also thank P. Tarasov and another anonymous reviewer as well as the editor Jan A. Piotrowski for their constructive comments. Proxy data of core Co1412 are available via the PANGAEA data repository after publication. The authors have no conflict of

interest, financial or otherwise, to declare. Open access funding enabled and organized by Projekt DEAL.

Author contributions. – MMB, BW, HM, NL and LAP participated in the field campaign to Lake Emanda in 2017. LAP provided the infrastructure and BW led the combined seismic survey and sediment coring campaign. MMB conducted the data collection, processing and interpretation, provided most of the figures and took the lead in writing the manuscript. BW was involved in the discussion of the data and significantly helped with editing the manuscript. NL helped with core opening, documentation and description, took part in the scientific discussion and proofread the manuscript. HM contributed the carbon isotope data and the corresponding text passage in the ‘Material and methods’ section and provided valuable comments on the manuscript. ML provided the basis for Fig. 1. ML, GF and MM contributed to the interpretation of the data and did proofreading.

References

- Abbott, M. B. & Stafford, T. W. Jr 1996: Radiocarbon geochemistry of modern and ancient Arctic lake systems, Baffin Island, Canada. *Quaternary Research* 45, 300–311.
- Alekseev, M. N. 1997: Paleogeography and geochronology in the Russian eastern Arctic during the second half of the Quaternary. *Quaternary International* 41–42, 11–15.
- Alexanderson, H., Hjort, C., Möller, P., Antonov, O. & Pavlov, M. 2001: The North Taymyr ice-marginal zone, Arctic Siberia—a preliminary overview and dating. *Global and Planetary Change* 31, 427–445.
- Ananicheva, M. D. & Krenke, A. N. 2005: Evolution of climatic snow line and equilibrium line altitudes - North-Eastern Siberia mountains in the 20th century. *Ice and Climate News. The WCRP Climate and Cryosphere Newsletter* 6, 1–6.
- Andersen, K.K., Azuma, N., Barnola, J.M., Bigler, M., Biscaye, P., Caillon, N., Chappellaz, J., Clausen, H.B., Dahl-Jensen, D., Fischer, H., Fleckiger, J., Fritzsche, D., Fujii, Y., Goto-Azuma, K., Gr nvald, K., Gundestrup, N.S., Hansson, M., Huber, C., Hvidberg, C.S., Johnsen, S.J., Jonsell, U., Jouzel, J., Kipfstuhl, S., Landais, A., Leuenberger, M., Lorrain, R., Masson-Delmotte, V., Miller, H., Motoyama, H., Narita, H., Popp, T., Rasmussen, S.O., Raynaud, D., Rothlisberger, R., Ruth, U., Samyn, D., Schwander, J., Shoji, H., Siggard-Andersen, M.L., Steffensen, J.P., Stocker, T., Sveinbj-rnsdóttir, A.E., Svensson, A., Takata, M., Tison, J.L., Thorsteinsson, T., Watanabe, O., Wilhelms, F. & White, J.W.C. 2004: High-resolution record of Northern Hemisphere climate extending into the last interglacial period. *Nature* 431, 147–151.
- Anderson, P. M. & Lozhkin, A. V. 2001: The Stage 3 interstadial complex (Karginskii/middle Wisconsinan interval) of Beringia: variations in paleoenvironments and implications for paleoclimatic interpretations. *Quaternary Science Reviews* 20, 93–125.
- Anderson, P. M., Lozhkin, A. V. & Brubaker, L. B. 2002: Implications of a 24,000-yr palynological record for a Younger Dryas cooling and for boreal forest development in northeastern Siberia. *Quaternary Research* 57, 325–333.
- Andreev, A. A. & Tarasov, P. E. 2013: Pollen records, postglacial: Northern Asia. In Elias, S. A. & Mock, C. J. (eds.): *Encyclopedia of Quaternary Science*, 164–172. Elsevier, Amsterdam.
- Andreev, A. A., Grosse, G., Schirrmeister, L., Kuznetsova, T. V., Kuzmina, S. A., Bobrov, A. A., Tarasov, P. E., Novenko, E. Y., Meyer, H., Derevyagin, A. Y., Kienast, F., Bryantseva, A. & Kunitsky, V. V. 2009: Weichselian and Holocene palaeoenvironmental history of the Bol’shoy Lyakhovsky Island, New Siberian Archipelago, Arctic Siberia. *Boreas* 38, 72–110.
- Andreev, A. A., Klimanov, V. A. & Sulerzhitsky, L. D. 1997: Younger Dryas pollen records from central and southern Yakutia. *Quaternary International* 41–42, 111–117.
- Andreev, A. A., Schirrmeister, L., Siegert, C., Bobrov, A., Demske, D., Seiffert, M. & Hubberten, H.-W. 2002: Paleoenvironmental changes in northeastern Siberia during the Late Quaternary - Evidence from pollen records of the Bykovsky Peninsula. *Polarforschung* 70, 13–25.

- Andreev, A. A., Schirrmeister, L., Tarasov, P. E., Ganopolski, A., Brovkin, V., Siebert, C., Wetterich, S. & Hubberten, H.-W. 2011: Vegetation and climate history in the Laptev Sea region (Arctic Siberia) during Late Quaternary inferred from pollen records. *Quaternary Science Reviews* 30, 2182–2199.
- Andreev, A. A., Tarasov, P., Schwamborn, G., Ilyashuk, B., Ilyashuk, E., Bobrov, A., Klimanov, V., Rachold, V. & Hubberten, H.-W. 2004: Holocene paleoenvironmental records from Nikolay Lake, Lena River Delta, Arctic Russia. *Palaeogeography, Palaeoclimatology, Palaeoecology* 209, 197–217.
- Ariztegui, D. & McKenzie, J. A. 1995: Temperature-dependent carbon-isotope fractionation of organic matter: a potential paleoclimatic indicator in Holocene lacustrine sequences. In Frenzel, B., Stauffer, B. & Weiss, M. M. (eds.): *Problems of Stable Isotopes in Tree-Rings, Lake Sediments and Peat-Bogs as Climatic Evidence for the Holocene*, 7–28. Gustav Fischer Verlag, Stuttgart.
- Arnaud, F., Révillon, S., Debret, M., Revel, M., Chapron, E., Jacob, J., Giguët-Covex, C., Poulénard, J. & Magny, M. 2012: Lake Bourget regional erosion patterns reconstruction reveals Holocene NW European Alps soil evolution and paleohydrology. *Quaternary Science Reviews* 51, 81–92.
- Ashastina, K., Kuzmina, S., Rudaya, N., Troeva, E., Schoch, W. H., Römermann, C., Reinecke, J., Otte, V., Savvinov, G., Wesche, K. & Kienast, F. 2018: Woodlands and steppes: Pleistocene vegetation in Yakutia's most continental part recorded in the Batagay permafrost sequence. *Quaternary Science Reviews* 196, 38–61.
- Ashastina, K., Schirrmeister, L., Fuchs, M. & Kienast, F. 2017: Palaeoclimate characteristics in interior Siberia of MIS 6–2: first insights from the Batagay permafrost mega-thaw slump in the Yana Highlands. *Climate of the Past* 13, 795–818.
- Balascio, N. L. & Bradley, R. S. 2012: Evaluating Holocene climate change in northern Norway using sediment records from two contrasting lake systems. *Journal of Paleolimnology* 48, 259–273.
- Barr, I. D. & Clark, C. D. 2012: Late Quaternary glaciations in Far NE Russia; combining moraines, topography and chronology to assess regional and global glaciation synchrony. *Quaternary Science Reviews* 53, 72–87.
- Berger, A. & Loutre, M.-F. 1991: Insolation values for the climate of the last 10 million years. *Quaternary Science Reviews* 10, 297–317.
- Berner, R. A. 1981: A new geochemical classification of sedimentary environments. *Journal of Sedimentary Petrology* 51, 359–366.
- Bezrukova, E. V., Tarasov, P. E., Solovieva, N., Krivonogov, S. K. & Riedel, F. 2010: Last glacial–interglacial vegetation and environmental dynamics in southern Siberia: Chronology, forcing and feedbacks. *Palaeogeography, Palaeoclimatology, Palaeoecology* 296, 185–198.
- Biskaborn, B. K., Subetto, D. A., Savelieva, L. A., Vakhrameeva, P. S., Hansche, A., Herzsuh, U., Klemm, J., Heinecke, L., Pestryakova, L. A., Meyer, H., Kuhn, G. & Diekmann, B. 2016: Late Quaternary vegetation and lake system dynamics in north-eastern Siberia: implications for seasonal climate variability. *Quaternary Science Reviews* 147, 406–421.
- Björck, S. & Wohlfarth, B. 2002: ¹⁴C chronostratigraphic techniques in paleolimnology. In Last, W. M. & Smol, J. P. (eds.): *Tracking Environmental Change Using Lake Sediments. Basin Analysis, Coring, and Chronological Techniques*, 205–245. Springer, Dordrecht.
- Blaauw, M. & Christen, J. A. 2011: Flexible paleoclimate age-depth models using an autoregressive gamma process. *Bayesian Analysis* 6, 457–474.
- Blott, S. J. & Pye, K. 2001: GRADISTAT: a grain size distribution and statistics package for the analysis of unconsolidated sediments. *Earth Surface Processes and Landforms* 26, 1237–1248.
- Bonne, J. L., Meyer, H., Behrens, M., Boike, J., Kipfstuhl, S., Rabe, B., Schmidt, T., Schönicke, L., Steen-Larsen, H. C. & Werner, M. 2020: In review: Moisture origin as a driver of temporal variabilities of the water vapour isotopic composition in the Lena River Delta, Siberia. *Atmospheric Chemistry and Physics Discussions* 20, 10493–10511, <https://doi.org/10.5194/acp-2019-942>.
- Boyle, J. F. 2002: Inorganic geochemical methods in palaeolimnology. In Last, W. M. & Smol, J. P. (eds.): *Tracking Environmental Change Using Lake Sediments. Physical and Geochemical Methods*, 83–141. Springer, Dordrecht.
- Brigham-Grette, J., Lozhkin, A. V., Anderson, P. M. & Glushkova, O. Y. 2004: Paleoenvironmental conditions in western Beringia before and during the Last Glacial Maximum. In Madsen, D. B. (ed.): *Entering America: Northeast Asia and Beringia Before The Last Glacial Maximum*, 29–61. University of Utah Press, Salt Lake City.
- Clark, P. U., Dyke, A. S., Shakun, J. D., Carlson, A. E., Clark, J., Wohlfarth, B., Mitrovica, J. X., Hostetler, S. W. & McCabe, A. M. 2009: The Last Glacial Maximum. *Science* 325, 710–714.
- Claussen, M., Ganopolski, A., Brovkin, V., Gerstengarbe, F. & Werner, P. 2003: Simulated global-scale response of the climate system to Dansgaard/Oeschger and Heinrich events. *Climate Dynamics* 21, 361–370.
- Cohen, A. S. 2003: *Paleolimnology: The History and Evolution of Lake Systems*. 528 pp. Oxford University Press, New York.
- Dale Guthrie, R. 2001: Origin and causes of the mammoth steppe: a story of cloud cover, woolly mammal tooth pits, buckles, and inside-out Beringia. *Quaternary Science Reviews* 20, 549–574.
- Davies, S. J., Lamb, H. F. & Roberts, S. J. 2015: Micro-XRF core scanning in palaeolimnology: recent developments. In Croudace, I. W. & Rothwell, R. G. (eds.): *Micro-XRF Studies of Sediment Cores*, 189–226. Springer, Dordrecht.
- Davison, W. 1993: Iron and manganese in lakes. *Earth-Science Reviews* 34, 119–163.
- Demske, D., Heumann, G., Granoszewski, W., Nita, M., Mamakowa, K., Tarasov, P. E. & Oberhänsli, H. 2005: Late glacial and Holocene vegetation and regional climate variability evidenced in high-resolution pollen records from Lake Baikal. *Global and Planetary Change* 46, 255–279.
- Dewald, A., Heinze, S., Jolie, J., Zilges, A., Dunai, T., Rethemeyer, J., Melles, M., Staubwasser, M., Kuczewski, B., Richter, J., Radtke, U., von Blanckenburg, F. & Klein, M. 2013: CologneAMS, a dedicated center for accelerator mass spectrometry in Germany. *Nuclear Instruments and Methods in Physics Research Section B: Beam Interactions with Materials and Atoms* 294, 18–23.
- Diekmann, B., Pestryakova, L., Nazarova, L., Subetto, D., Tarasov, P. E., Stauch, G., Thiemann, A., Lehmkuhl, F., Biskaborn, B. & Kuhn, G. 2017: Late Quaternary lake dynamics in the Verkhojansk Mountains of Eastern Siberia: implications for climate and glaciation history. *Polarforschung* 86, 97–110.
- Dushin, V. A., Serdyukova, O. P., Malyugin, A. A., Nikulina, I. A., Kozmin, V. S., Burmako, P. L., Abaturova, I. V. & Kozmina, L. I. 2009: *State Geological Map of the Russian Federation 1:200 000. Sheet Q42I, II*. VSEGEI, St. Petersburg (in Russian).
- Elias, S. A. & Brigham-Grette, J. 2013: GLACIATIONS; Late Pleistocene glacial events in Beringia. In Elias, S. A. & Mock, C. J. (eds.): *Encyclopedia of Quaternary Science*, 191–201. Elsevier, Amsterdam.
- Francke, A., Dosseto, A., Panagiotopoulos, K., Leicher, N., Lacey, J. H., Kyrikou, S., Wagner, B., Zanchetta, G., Kouli, K. & Leng, M. J. 2019: Sediment residence time reveals Holocene shift from climatic to vegetation control on catchment erosion in the Balkans. *Global and Planetary Change* 177, 186–200.
- Francke, A., Wagner, B., Just, J., Leicher, N., Gromig, R., Baumgarten, H., Vogel, H., Lacey, J. H., Sadori, L., Wonik, T., Leng, M. J., Zanchetta, G., Sulpizio, R. & Giaccio, B. 2016: Sedimentological processes and environmental variability at Lake Ohrid (Macedonia, Albania) between 637 ka and the present. *Biogeosciences* 13, 1179–1196.
- Francke, A., Wennrich, V., Sauerbrey, M., Juschus, O., Melles, M. & Brigham-Grette, J. 2013: Multivariate statistic and time series analyses of grain-size data in Quaternary sediments of Lake El'gygytyn, NE Russia. *Climate of the Past* 9, 2459–2470.
- Gebhardt, A. C., Naudts, L., De Mol, L., Klerkx, J., Abdrakhmatov, K., Sobel, E. R. & De Batist, M. 2017: High-amplitude lake-level changes in tectonically active Lake Issyk-Kul (Kyrgyzstan) revealed by high-resolution seismic reflection data. *Climate of the Past* 13, 73–92.
- Glushkova, O. Y. 2011: Chapter 63 - Late Pleistocene glaciations in North-East Asia. In Ehlers, J., Gibbard, P. L. & Hughes, P. D. (eds.): *Developments in Quaternary Science*, 865–875. Elsevier, Amsterdam.
- Gorbarenko, S. A., Southon, J. R., Keigwin, L. D., Cherepanova, M. V. & Gvozdeva, I. G. 2004: Late Pleistocene-Holocene oceanographic variability in the Okhotsk Sea: geochemical, lithological and

- paleontological evidence. *Palaeogeography, Palaeoclimatology, Palaeoecology* 209, 281–301.
- Hammarlund, D. 1993: A distinct $\delta^{13}\text{C}$ decline in organic lake sediments at the Pleistocene-Holocene transition in southern Sweden. *Boreas* 22, 236–243.
- Hua, Q., Barbetti, M. & Rakowski, A. Z. 2013: Atmospheric radiocarbon for the period 1950–2010. *Radiocarbon* 55, 2059–2072.
- Hughes, A. L. C., Gyllencreutz, R., Lohne, Ø. S., Mangerud, J. & Svendsen, J. I. 2016: The last Eurasian ice sheets – a chronological database and time-slice reconstruction, DATED-1. *Boreas* 45, 1–45.
- Kienast, F., Schirmer, L., Siegert, C. & Tarasov, P. 2005: Palaeobotanical evidence for warm summers in the East Siberian Arctic during the last cold stage. *Quaternary Research* 63, 283–300.
- Kind, N. V. 1975: Glaciations in the Verkhoyansk Mountains and their place in the radiocarbon chronology of the Late Pleistocene Anthropogene. *Biuletyn Peryglacjalny* 24, 41–54.
- Knies, J., Nowaczyk, N., Müller, C., Vogt, C. & Stein, R. 2000: A multiproxy approach to reconstruct the environmental changes along the Eurasian continental margin over the last 150 000 years. *Marine Geology* 163, 317–344.
- Kolpakov, V. V. & Belova, A. P. 1980: Radiocarbon dating in the glacial region of Verkhoyan'ye and its framing. In Ivanova, I. K. & Kind, N. V. (eds.): *Geochronology of the Quaternary Period*, 230–235. Nauka, Moscow (in Russian).
- Köppen, W. 2011: The thermal zones of the earth according to the duration of hot, moderate and cold periods and to the impact of heat on the organic world. Translated from German and edited by Volken, E. & Brönnimann, S. *Meteorologische Zeitschrift* 20, 351–360.
- Koreisha, M. M. 1991: *Glaciation of the Verkhoyansk-Kolyma Region*. 114 pp. Nauka. Academy of Sciences of the USSR Soviet Geophysical Committee, Moscow (in Russian).
- Krinner, G., Diekmann, B., Colleoni, F. & Stauch, G. 2011: Global, regional and local scale factors determining glaciation extent in Eastern Siberia over the last 140,000 years. *Quaternary Science Reviews* 30, 821–831.
- Lambeck, K., Yokoyama, Y. & Purcell, T. 2002: Into and out of the Last Glacial Maximum: sea-level change during Oxygen Isotope Stages 3 and 2. *Quaternary Science Reviews* 21, 343–360.
- Laskar, J., Robutel, P., Joutel, F., Gastineau, M., Correia, A. C. M. & Levrard, B. 2004: A long-term numerical solution for the insolation quantities of the Earth. *Astronomy & Astrophysics* 428, 261–285.
- Lebas, E., Krastel, S., Wagner, R., Gromig, R., Fedorov, G., Baumer, M., Kostromina, N. & Haflidason, H. 2019: Seismic stratigraphical record of Lake Levinson-Lessing, Taymyr Peninsula: evidence for ice-sheet dynamics and lake-level fluctuations since the Early Weichselian. *Boreas* 48, 470–487.
- Lisiecki, L. E. & Raymo, M. E. 2005: A Plio-Pleistocene stack of 57 globally distributed benthic $\delta^{18}\text{O}$ records. *Paleoceanography* 20, 1–17. PA1003, <https://doi.org/10.1029/2004PA001071>.
- Löwemark, L., Chen, H. F., Yang, T. N., Kylander, M., Yu, E. F., Hsu, Y. W., Lee, T. Q., Song, S. R. & Jarvis, S. 2011: Normalizing XRF-scanner data: a cautionary note on the interpretation of high-resolution records from organic-rich lakes. *Journal of Asian Earth Sciences* 40, 1250–1256.
- Lozhkin, A. V. & Anderson, P. M. 2011: Forest or no forest: implications of the vegetation record for climatic stability in Western Beringia during Oxygen Isotope Stage 3. *Quaternary Science Reviews* 30, 2160–2181.
- Lozhkin, A. V., Anderson, P. M., Matrosova, T. V. & Minyuk, P. S. 2007: The pollen record from El'gygytgyn Lake: implications for vegetation and climate histories of northern Chukotka since the late middle Pleistocene. *Journal of Paleolimnology* 37, 135–153.
- Mayr, C., Lücke, A., Maidana, N. I., Wille, M., Haberzettl, T., Corbella, H., Ohlendorf, C., Schäbitz, F., Fey, M., Janssen, S. & Zolitschka, B. 2009: Isotopic fingerprints on lacustrine organic matter from Laguna Potrok Aike (southern Patagonia, Argentina) reflect environmental changes during the last 16,000 years. *Journal of Paleolimnology* 42, 81–102.
- Meyer, H., Derevyagin, A. Y., Siegert, C. & Hubberten, H.-W. 2002: Paleoclimate studies on Bykovsky Peninsula, North Siberia-hydrogen and oxygen isotopes in ground ice. *Polarforschung* 70, 37–51.
- Meyers, P. A. 1997: Organic geochemical proxies of paleoceanographic, paleolimnologic, and paleoclimatic processes. *Organic Geochemistry* 27, 213–250.
- Meyers, P. A. 2003: Applications of organic geochemistry to paleolimnological reconstructions: a summary of examples from the Laurentian Great Lakes. *Organic Geochemistry* 34, 261–289.
- Meyers, P. A. & Ishiwatari, R. 1993: Lacustrine organic geochemistry—an overview of indicators of organic matter sources and diagenesis in lake sediments. *Organic Geochemistry* 20, 867–900.
- Meyers, P. A. & Teranes, J. L. 2001: Sediment organic matter. In Last, W. M. & Smol, J. P. (eds.): *Tracking Environmental Change Using Lake Sediments. Physical and Geochemical Methods*, 239–270. Springer, Dordrecht.
- Müller, A. 2001: Late- and postglacial sea-level change and paleoenvironments in the Oder Estuary, Southern Baltic Sea. *Quaternary Research* 55, 86–96.
- Müller, S., Tarasov, P. E., Andreev, A. A. & Diekmann, B. 2009: Late Glacial to Holocene environments in the present-day coldest region of the Northern Hemisphere inferred from a pollen record of Lake Billyakh, Verkhoyansk Mts, NE Siberia. *Climate of the Past* 5, 73–84.
- Müller, S., Tarasov, P. E., Andreev, A. A., Tütken, T., Gartz, S. & Diekmann, B. 2010: Late Quaternary vegetation and environments in the Verkhoyansk Mountains region (NE Asia) reconstructed from a 50-kyr fossil pollen record from Lake Billyakh. *Quaternary Science Reviews* 29, 2071–2086.
- Murton, J. B., Goslar, T., Edwards, M. E., Bateman, M. D., Danilov, P. P., Savvinov, G. N., Gubin, S. V., Ghaleb, B., Haile, J., Kanevskiy, M., Lozhkin, A. V., Lupachev, A. V., Murton, D. K., Shur, Y., Tikhonov, A., Vasil'chuk, A. C., Vasil'chuk, Y. K. & Wolfe, S. A. 2015: Palaeoenvironmental interpretation of Yedomia Silt (ice complex) deposition as cold-climate loess, Duvanny Yar, Northeast Siberia. *Permafrost and Periglacial Processes* 26, 208–288.
- New, M., Lister, D., Hulme, M. & Makin, I. 2002: A high-resolution data set of surface climate over global land areas. *Climate Research* 21, 1–25. Data available at <http://wcatlas.iwmi.org> (accessed 05.05.2020).
- Opel, T., Murton, J. B., Wetterich, S., Meyer, H., Ashastina, K., Günther, F., Grotheer, H., Mollenhauer, G., Danilov, P. P., Boeskorov, V., Savvinov, G. N. & Schirmer, L. 2019: Past climate and continentality inferred from ice wedges at Batagay megaslump in the Northern Hemisphere's most continental region, Yana Highlands, interior Yakutia. *Climate of the Past* 15, 1443–1461.
- Oxman, V. S. 2003: Tectonic evolution of the Mesozoic Verkhoyansk-Kolyma belt (NE Asia). *Tectonophysics* 365, 45–76.
- Papina, T., Malygina, N., Eirikh, A., Galanin, A. & Zheleznyak, M. 2017: Isotopic composition and sources of atmospheric precipitation in central Yakutia. *Earth's Cryosphere* 21, 52–61.
- Parfenov, L. M. 1991: Tectonics of the Verkhoyansk-Kolyma Mesozooids in the context of plate-tectonics. *Tectonophysics* 199, 319–342.
- Penland, S. & Kulp, M. A. 2005: Deltas. In Schwartz, M. L. (ed.): *Encyclopedia of Coastal Science*, 362–368. Springer, Dordrecht.
- Pisaric, M. F. J., MacDonald, G. M., Velichko, A. A. & Cwynar, L. C. 2001: The Lateglacial and Postglacial vegetation history of the northwestern limits of Beringia, based on pollen, stomate and tree stump evidence. *Quaternary Science Reviews* 20, 235–245.
- Popp, S., Belolyubsky, I., Lehmkuhl, F., Prokopiev, A., Siegert, C., Spektor, V., Stauch, G. & Diekmann, B. 2007: Sediment provenance of late Quaternary morainic, fluvial and loess-like deposits in the southwestern Verkhoyansk Mountains (Eastern Siberia) and implications for regional palaeoenvironmental reconstructions. *Geological Journal* 42, 477–497.
- Prokopenko, A. A., Williams, D. F., Karabanov, E. B. & Khursevich, G. K. 2001: Continental response to Heinrich events and Bond cycles in sedimentary record of Lake Baikal, Siberia. *Global and Planetary Change* 28, 217–226.
- Rasmussen, S. O., Andersen, K. K., Svensson, A. M., Steffensen, J. P., Vinther, B. M., Clausen, H. B., Siggaard-Andersen, M. L., Johnsen, S. J., Larsen, L. B., Dahl-Jensen, D., Bigler, M., Röthlisberger, R., Fischer, H., Goto-Azuma, K., Hansson, M. E. & Ruth, U. 2006: A new Greenland ice core chronology for the last glacial termination. *Journal of Geophysical Research: Atmospheres* 111, 1–16. D06102, <https://doi.org/10.1029/2005JD006079>.

- Reimer, P. J., Bard, E., Bayliss, A., Beck, J. W., Blackwell, P. G., Ramsey, C. B., Buck, C. E., Cheng, H., Edwards, R. L., Friedrich, M., Grootes, P. M., Guilderson, T. P., Haflidason, H., Hajdas, I., Hatté, C., Heaton, T. J., Hoffmann, D. L., Hogg, A. G., Hughen, K. A., Kaiser, K. F., Kromer, B., Manning, S. W., Niu, M., Reimer, R. W., Richards, D. A., Scott, E. M., Southon, J. R., Staff, R. A., Turney, C. S. M. & van der Plicht, J. 2013: IntCal13 and Marine13 radiocarbon age calibration curves 0–50,000 years cal BP. *Radiocarbon* 55, 1869–1887.
- Renssen, H., Seppä, H., Crosta, X., Goosse, H. & Roche, D. M. 2012: Global characterization of the Holocene Thermal Maximum. *Quaternary Science Reviews* 48, 7–19.
- Renssen, H., Seppä, H., Heiri, O., Roche, D. M., Goosse, H. & Fichetef, T. 2009: The spatial and temporal complexity of the Holocene thermal maximum. *Nature Geoscience* 2, 411–414.
- Rethemeyer, J., Fülöp, R. H., Höfle, S., Wacker, L., Heinze, S., Hajdas, I., Patt, U., König, S., Stapper, B. & Dewald, A. 2013: Status report on sample preparation facilities for ^{14}C analysis at the new CologneAMS center. *Nuclear Instruments and Methods in Physics Research Section B: Beam Interactions with Materials and Atoms* 294, 168–172.
- Rothacker, L., Dreves, A., Sirocko, F., Grootes, P. M. & Nadeau, M.-J. 2013: Dating bulk sediments from limnic deposits using a grain-size approach. *Radiocarbon* 55, 943–950.
- Schirrmeister, L., Grosse, G., Schwamborn, G., Andreev, A. A., Meyer, H., Kunitsky, V. V., Kuznetsova, T. V., Dorozhkina, M. V., Pavlova, E. Y., Bobrov, A. A. & Oezen, D. 2003: Late Quaternary history of the accumulation plain north of the Chekanovsky Ridge (Lena Delta, Russia): a multidisciplinary approach. *Polar Geography* 27, 277–319.
- Schirrmeister, L., Schwamborn, G., Overduin, P. P., Strauss, J., Fuchs, M. C., Grigoriev, M., Yakshina, I., Rethemeyer, J., Dietze, E. & Wetterich, S. 2017: Yedoma Ice Complex of the Buor Khaya Peninsula (southern Laptev Sea). *Biogeosciences* 14, 1261–1283.
- Sher, A. V., Kuzmina, S. A., Kuznetsova, T. V. & Sulerzhitsky, L. D. 2005: New insights into the Weichselian environment and climate of the East Siberian Arctic, derived from fossil insects, plants, and mammals. *Quaternary Science Reviews* 24, 533–569.
- Sirocko, F., Dietrich, S., Veres, D., Grootes, P. M., Schaber-Mohr, K., Seelos, K., Nadeau, M.-J., Kromer, B., Rothacker, L., Röhner, M., Krbetschek, M., Appleby, P., Hambach, U., Rolf, C., Sudo, M. & Grim, S. 2013: Multi-proxy dating of Holocene maar lakes and Pleistocene dry maar sediments in the Eifel, Germany. *Quaternary Science Reviews* 62, 56–76.
- Stauch, G. 2006: *Jungquartäre Landschaftsentwicklung im Werchhoyansk Gebirge, Nordost Sibirien (Late Quaternary landscape development in the Verkhoyansk Mountains, North-Eastern Siberia)*. 176 pp. Geographisches Institut der RWTH Aachen, Aachen (in German).
- Stauch, G. & Gualtieri, L. 2008: Late Quaternary glaciations in northeastern Russia. *Journal of Quaternary Science* 23, 545–558.
- Stauch, G. & Lehmkuhl, F. 2010: Quaternary glaciations in the Verkhoyansk Mountains, Northeast Siberia. *Quaternary Research* 74, 145–155.
- Stauch, G. & Lehmkuhl, F. 2011: Extent and timing of Quaternary glaciations in the Verkhoyansk Mountains. In Ehlers, P., Gibbard, P. L. & Hughes, P. D. (eds.): *Quaternary Glaciations - Extent and Chronology - A Closer Look*, 877–881. Elsevier, Amsterdam.
- Stauch, G., Lehmkuhl, F. & Frechen, M. 2007: Luminescence chronology from the Verkhoyansk Mountains (North-Eastern Siberia). *Quaternary Geochronology* 2, 255–259.
- Stephanova, N. A. 1958: On the lowest temperatures on earth. *Monthly Weather Review* 86, 6–10.
- Stewart, B. A. & Hartge, K. H. 1995: *Soil Structure: Its Development and Function*. 448 pp. CRC Press, Florida.
- Stuiver, M., Reimer, P. J. & Reimer, R. W. 2020: *CALIB 7.1*. Available at: <http://calib.org> (accessed 23.04.2020).
- Subetto, D. A., Nazarova, L. B., Pestryakova, L. A., Syrykh, L. S., Andronikov, A. V., Biskaborn, B., Diekmann, B., Kuznetsov, D. D., Sapelko, T. V. & Grekov, I. M. 2017: Paleolimnological studies in Russian northern Eurasia: a review. *Contemporary Problems of Ecology* 10, 327–335.
- Svendsen, J. I., Alexanderson, H., Astakhov, V. I., Demidov, I., Dowdeswell, J. A., Funder, S., Gataullin, V., Henriksen, M., Hjort, C., Houmark-Nielsen, M., Hubberten, H. W., Ingólfsson, Ó., Jakobsson, M., Kjær, K. H., Larsen, E., Lokrantz, H., Lunkka, J. P., Lysä, A., Mangerud, J., Matiouchkov, A., Murray, A., Möller, P., Niessen, F., Nikolskaya, O., Polyak, L., Saarnisto, M., Siegert, C., Siegert, M. J., Spielhagen, R. F. & Stein, R. 2004: Late Quaternary ice sheet history of northern Eurasia. *Quaternary Science Reviews* 23, 1229–1271.
- Svendsen, J. I., Færseth, L. M. B., Gyllencreutz, R., Haflidason, H., Henriksen, M., Hovland, M. N., Lohne, Ø. S., Mangerud, J., Nazarov, D., Regnell, C. & Schaefer, J. M. 2019: Glacial and environmental changes over the last 60 000 years in the Polar Ural Mountains, Arctic Russia, inferred from a high-resolution lake record and other observations from adjacent areas. *Boreas* 48, 407–431.
- Svendsen, J. I., Kruger, L. C., Mangerud, J., Astakhov, V. I., Paus, A., Nazarov, D. & Murray, A. 2014: Glacial and vegetation history of the Polar Ural Mountains in northern Russia during the Last Ice Age, Marine Isotope Stages 5–2. *Quaternary Science Reviews* 92, 409–428.
- Swann, G. E. A., Leng, M. J., Juschus, O., Melles, M., Brigham-Grette, J. & Sloane, H. J. 2010: A combined oxygen and silicon diatom isotope record of Late Quaternary change in Lake El'gygytyn, North East Siberia. *Quaternary Science Reviews* 29, 774–786.
- Tarasov, P. E., Ilyashuk, B. P., Leipe, C., Müller, S., Plessen, B., Hoelzmann, P., Kostrova, S. S., Bezrukova, E. V. & Meyer, H. 2019: Insight into the Last Glacial Maximum climate and environments of the Baikal region. *Boreas* 48, 488–506.
- Tarasov, P. E., Müller, S., Zech, M., Andreeva, D., Diekmann, B. & Leipe, C. 2013: Last glacial vegetation reconstructions in the extreme-continental eastern Asia: potentials of pollen and n-alkane biomarker analyses. *Quaternary International* 290–291, 253–263.
- Turney, C. S. M. 1999: Lacustrine bulk organic $\delta^{13}\text{C}$ in the British Isles during the Last Glacial-Holocene transition (14–9 ka ^{14}C BP). *Arctic, Antarctic, and Alpine Research* 31, 71–81.
- Urban, N. R., Ernst, K. & Bernasconi, S. 1999: Addition of sulfur to organic matter during early diagenesis of lake sediments. *Geochimica et Cosmochimica Acta* 63, 837–853.
- Vasil'chuk, Y. K. 2006: *Syngenetic Ice Wedges: Cyclical Formation, Radiocarbon Age and Stable Isotope Records*. 404 pp. Moscow University Press, Moscow.
- Voelker, A. H. L. 2002: Global distribution of centennial-scale records for Marine Isotope Stage (MIS) 3: a database. *Quaternary Science Reviews* 21, 1185–1212.
- Wagner, B., Lotter, A. F., Nowaczyk, N., Reed, J. M., Schwab, A., Sulpizio, R., Valsecchi, V., Wessels, M. & Zanchetta, G. 2009: A 40,000-year record of environmental change from ancient Lake Ohrid (Albania and Macedonia). *Journal of Paleolimnology* 41, 407–430.
- Wagner, B., Melles, M., Hahne, J., Niessen, F. & Hubberten, H.-W. 2000: Holocene climate history of Geographical Society Ø, East Greenland — evidence from lake sediments. *Palaeogeography, Palaeoclimatology, Palaeoecology* 160, 45–68.
- Wang, Y. J., Cheng, H., Edwards, R. L., An, Z. S., Wu, J. Y., Shen, C. C. & Dorale, J. A. 2001: A high-resolution absolute-dated Late Pleistocene monsoon record from Hulu Cave, China. *Science* 294, 2345–2348.
- Werner, K., Tarasov, P. E., Andreev, A. A., Müller, S., Kienast, F., Zech, M., Zech, W. & Diekmann, B. 2010: A 12.5-kyr history of vegetation dynamics and mire development with evidence of Younger Dryas larch presence in the Verkhoyansk Mountains, East Siberia Russia. *Boreas* 39, 56–68.
- Yi, S., Wischnewski, K., Langer, M., Muster, S. & Boike, J. 2014: Freeze/thaw processes in complex permafrost landscapes of northern Siberia simulated using the TEM ecosystem model: impact of thermokarst ponds and lakes. *Geoscientific Model Development* 7, 1671–1689.
- Zanina, O. G., Gubin, S. V., Kuzmina, S. A., Maximovich, S. V. & Lopatina, D. A. 2011: Late-Pleistocene (MIS 3–2) palaeoenvironments as recorded by sediments, palaeosols, and ground-squirrel nests at Duvanny Yar, Kolyma lowland, northeast Siberia. *Quaternary Science Reviews* 30, 2107–2123.
- Zech, W., Zech, R., Zech, M., Leiber, K., Dippold, M., Frechen, M., Bussert, R. & Andreev, A. 2011: Obliquity forcing of Quaternary

glaciation and environmental changes in NE Siberia. *Quaternary International* 234, 133–145.

Zhigarev, L. A. & Bocharova, I. S. 1978: A comparative description of the composition and properties of the lacustrine alluvial deposits of

northwestern Siberia and the Yana-Indigirka Lowland, considered in the light of cryolithogenesis. In Sanger, F. J. & Hyde, P. J. (eds.): *Permafrost: Second International Conference*, July 13–28 1973, 124–126. National Academy of Science, Washington.